Inorg. Chem. **2009**, *48*, 3420−3437

Forum

Slow Dynamics of the Magnetization in One-Dimensional Coordination Polymers: Single-Chain Magnets

Hitoshi Miyasaka,*,† Miguel Julve,*,‡ Masahiro Yamashita,† and Rodolphe Clérac*,§,||

Department of Chemistry, Graduate School of Science, Tohoku University, 6-3 Aramaki-Aza-Aoba, Aoba-ku, Sendai, Miyagi 980-8578, Japan, Departament de Química Inorgànica, Instituto de Ciencia Molecular (ICMol), Universitat de València, Polígono La Coma s/n, Paterna, València E-46980, Spain, CNRS, UPR 8641, Centre de Recherche Paul Pascal (CRPP), Equipe "Matériaux Moléculaires Magnétiques", 115 avenue du Dr. Albert Schweitzer, Pessac F-33600, France, and Université de Bordeaux, UPR 8641, Pessac F-33600, France

Received October 25, 2008

Slow relaxation of the magnetization (i.e., "magnet-like" behavior) in materials composed of magnetically isolated chains was observed for the first time in 2001. This type of behavior was predicted in the 1960s by Glauber in a chain of ferromagnetically coupled Ising spins (the so-called Glauber dynamics). In 2002, this new class of nanomagnets was named single-chain magnets (SCMs) by analogy to single-molecule magnets that are isolated molecules displaying related superparamagnetic properties. A long-range order occurs only at $T = 0$ K in any pure one-dimensional (1D) system, and thus such systems remain in their paramagnetic state at any finite temperature. Nevertheless, the combined action of large uniaxial anisotropy and intrachain magnetic interactions between high-spin magnetic units of the 1D arrangement promotes long relaxation times for the magnetization reversal with decreasing temperature, and finally at significantly low temperatures, the material can behave as a magnet. In this Forum Article, we summarize simple theoretical approaches used for understanding typical SCM behavior and some rational synthetic strategies to obtain SCM materials together with representative examples of SCMs previously reported.

I. Introduction

Single-chain magnets (SCMs) are made up of magnetically isolated chains possessing a finite magnetization that can be frozen in the absence of an applied magnetic field. At low temperatures, the relaxation of the magnetization becomes so slow that these systems can be considered as a magnet. These two sentences are the simplest way to define a SCM system. A purely one-dimensional (1D) system does not exhibit any long-range ordering at a finite temperature, and therefore it cannot stabilize a "thermodynamic magnet", resulting, for example, from a ferromagnetic order.[1] Nevertheless, it is possible in *special cases* to obtain a magnet behavior using a frozen situation of the magnetization in a 1D system that exhibits a very slow relaxation at a finite temperature. In 1963, R. J. Glauber predicted that chains of ferromagnetically coupled *Ising* spins should display slow relaxation of the magnetization;[2] since this work, this phenomenon has been called the Glauber dynamics and has been discussed for a long time mainly in the field of physics. In this respect, the report from Gambardella et al. in 2002 provided us with important information on the chain magnetism: these authors have shown that an isolated chain

* To whom correspondence should be addressed. E-mail: miyasaka@agnus.chem.tohoku.ac.jp (H.M.), miguel.julve@uv.es (M.J.), clerac@crpp-bordeaux.cnrs.fr (R.C.). Fax: +81 22 795 6548 (H.M.), +34 96 354 3273 (M.J.), +33 5 56 84 56 00 (R.C.).
† Tohoku University.
‡ Universitat de València.
§ CNRS, UPR 8641, Centre de Recherche Paul Pascal (CRPP).
|| Université de Bordeaux.

(1) (a) Landau, L. D.; Lifshitz, E. M. *Stat. Phys.* **1959**, *5*, 482. (b) Ising, E. *Z. Phys.* **1925**, *31*, 253. (c) Mermin, N. D.; Wagner, H. *Phys. Rev. Lett.* **1966**, *17*, 1133.
(2) Glauber, R. J. *J. Math. Phys.* **1963**, *4*, 294.

10.1021/ic802050j CCC: $40.75 © 2009 American Chemical Society
Published on Web 04/13/2009

of Co atoms arranged on a platinum vicinal surface exhibits ferromagnetism-like properties.[3] This system, which is the closest to the Glauber system, is certainly relevant to the SCM behavior observed in 1D coordination compounds described in this Forum Article, and it contributed to our understanding of the properties of the known Ising-type chains. In 2001, Gatteschi and co-workers reported the first observation of a slow relaxation of the magnetization in a cobalt(II)−organic radical alternating chain where the effective Ising-type spin $S_{\text{eff}} = {}^1/_2$ of Co^{II} ion and the isotropic $S = {}^1/_2$ of the radical are antiferromagnetically coupled.[4] At the same time, Miyasaka and Clérac discovered similar kinds of magnetic properties in chains of ferromagnetically coupled anisotropic $S = 3$ spin units.[5] The simplicity of these materials made of well-aligned Mn^{III} ions (possessing a finite uniaxial anisotropy) was the key to expand Glauber's theory and to investigate the magnetostructural correlations linked to the slow dynamics. Since then, these types of compounds have been named single-chain magnets by analogy to single-molecule magnets (SMMs) that are isolated molecules displaying related superparamagnetic properties.[6] Nowadays, this subject has become a hot topic of research at the frontier between chemistry and physics.[7,8] Although the known SCMs possess long relaxation times ($\tau >$ 1s) only at low temperatures (below ca. 10 K in most of the cases), the limitation to produce SCMs compatible with industrial applications seems less severe than that for SMMs. This remark is certainly one of the main reasons that explain why the chemistry and physics of these systems have become very active fields in the past seven years, during which SCM behavior in several compounds has been revealed. However, some fundamental questions beyond Glauber's theory dealing with the understanding of the relaxation mechanism in experimental SCM systems remain open.

From the definition on the SCM system given at the beginning of this section, the following three essential ingredients have to be controlled to design SCMs: (i) the noncancellation of the spin units along the chain, namely, preferring ferro- and ferrimagnetic spin organizations or canted antiferromagnetically arranged spins; (ii) the presence of a significant uniaxial anisotropy; (iii) the interchain interactions that must be as small as possible (in comparison to the intrachain ones). The two first points are directly connected to the nature of designed SCMs, whereas the latter one is a fundamental factor separating the superparamagnetism-like properties of the SCMs from the classical bulk three-dimensional order. In some cases, desired materials satisfying these ingredients may be serendipitously obtained, but their rational design together with the tuning of their individual intrinsic magnetic parameters are preferred when aiming at modeling the SCM behavior. Since the discovery of the first SCM material, a broad knowledge on these types of systems has been accumulated on the theoretical point of view as well as on the synthetic techniques to design them or related materials. This Forum Article summarizes both parts from the physics in order to understand SCM properties to the synthetic routes toward the rational design of SCMs. Its contents is organized as follows: after the present introduction (section I), the theoretical approaches that have been used to understand simple SCM behaviors will be described (section II); then, the rational synthetic strategies toward SCM systems (using SMMs, uniaxial anisotropic species, and metalloligands as building blocks) will be illustrated by selected examples (section III); finally, the last part will concern some perspectives and open questions in this young research field (section IV).

II. Simple Theoretical Approach on the SCM Properties

In the SCM systems, the first aspect of the theoretical analysis of magnetic properties is to understand the slow dynamics of the magnetization (i.e., during its return to the thermodynamic $M = 0$ state) by a study of the relaxation time and especially its temperature dependence. In the second time, it is important to check if the static magnetic properties are in agreement with 1D Ising or anisotropic Heisenberg models. Both analyses on dynamics and static experimental data are essential to conclude on the SCM behavior in a compound.[9]

II.1. Static Magnetic Properties: The Anisotropic Heisenberg Chain Model. Heisenberg and Ising chain models have been used extensively in theoretical works, but the study of real systems requires in most cases a more complicated Hamiltonian.[9] In most of the SCM examples reported in the literature (vide infra), the single-ion anisotropy is relevant and a finite magnetic anisotropy must be included in the model that leads to the following anisotropic Heisenberg Hamiltonian:

(3) Gambardella, P.; Dallmeyer, A.; Maiti, K.; Malagoli, M. C.; Eberhardt, W.; Kern, K.; Carbone, C. *Nature* **2002**, *416*, 301.

(4) Caneschi, A.; Gatteschi, D.; Lalioti, N.; Sangregorio, C.; Sessoli, R.; Venturi, G.; Vindigni, A.; Rettori, A.; Pini, M. G.; Novak, M. A. *Angew. Chem., Int. Ed.* **2001**, *40*, 1760.

(5) Clérac, R.; Miyasaka, H.; Yamashita, M.; Coulon, C. *J. Am. Chem. Soc.* **2002**, *124*, 12837.

(6) Reviews and book: (a) Gatteschi, D.; Caneschi, A.; Pardi, L.; Sessoli, R. *Science* **1994**, *265*, 1054. (b) Christou, G.; Gatteschi, D.; Hendrickson, D. N.; Sessoli, R. *MRS Bull.* **2000**, *25*, 66. (c) Gatteshi, D.; Sessoli, R. *Angew. Chem., Int. Ed.* **2003**, *42*, 268. (d) Gatteschi, D.; Sessoli, R.; Villain, J. *Molecular Nanomagnets*; Oxford University Press: Oxford, U.K., 2006.

(7) (a) Caneschi, A.; Gatteschi, D.; Lalioti, N.; Sangregorio, C.; Sessoli, R.; Venturi, G.; Vindigni, A.; Rettori, A.; Pini, M. G.; Novak, M. A. *Europhys. Lett.* **2002**, *58*, 771. (b) Bogani, L.; Caneschi, A.; Fedi, M.; Gatteschi, D.; Massi, M.; Novak, M. A.; Pini, M. G.; Rettori, A.; Sessoli, R.; Vindigni, A. *Phys. Rev. Lett.* **2004**, *92*, 207204. (c) Bogani, L.; Sessoli, R.; Pini, M. G.; Rettori, A.; Novak, M. A.; Rosa, P.; Massi, M.; Fedi, M.; Giuntini, L.; Caneschi, A.; Gatteschi, D. *Phys. Rev. B* **2005**, *72*, 064406. (d) Vindigni, A.; Rettori, A.; Bogani, L.; Caneschi, A.; Gatteschi, D.; Sessoli, R.; Novak, M. A. *Appl. Phys. Lett.* **2005**, *87*, 073102. (e) Vindigni, A.; Rettori, A.; Pini, M. G.; Carbone, C.; Gambardella, P. *Appl. Phys. A* **2006**, *82*, 385. (f) Bogani, L.; Vindigni, A.; Sessoli, R.; Gatteschi, D. *J. Mater. Chem.* **2008**, *18*, 4750.

(8) (a) Mito, M.; Deguchi, H.; Tajiri, T.; Takagi, S.; Yamashita, M.; Miyasaka, H. *Phys. Rev. B* **2005**, *72*, 144421. (b) Wernsdorfer, W.; Clérac, R.; Coulon, C.; Lecren, L.; Miyasaka, H. *Phys. Rev. Lett.* **2005**, *95*, 237203. (c) Oshima, Y.; Nojiri, H.; Asakura, K.; Sakai, T.; Yamashita, M.; Miyasaka, H. *Phys. Rev. B* **2006**, *73*, 214435. (d) Kishine, J.; Watanabe, T.; Deguchi, H.; Mito, M.; Sakai, T.; Tajiri, T.; Yamashita, M.; Miyasaka, H. *Phys. Rev. B* **2006**, *74*, 224419. (e) Coulon, C.; Clérac, R.; Wernsdorfer, W.; Colin, T.; Saitoh, A.; Motokawa, N.; Miyasaka, H. *Phys. Rev. B* **2007**, *76*, 214422.

(9) Coulon, C.; Miyasaka, H.; Clérac, R. *Struct. Bonding (Berlin)* **2006**, *122*, 163.

$$H = -2J\sum_{-\infty}^{+\infty}\vec{S}_i\vec{S}_{i+1} + D\sum_{-\infty}^{+\infty}\vec{S}_{iz}{}^2 \quad (1)$$

with J being the magnetic interaction between magnetic units of $\mathbf{S}_i$ spin along the chain, D the single-ion anisotropy of a magnetic $\mathbf{S}_i$ unit, and $\mathbf{S}_{iz}$ the z projection of the S_i spin. In 1975, Loveluck et al. described the magnetic properties deduced from this model.[10] In the case of uniaxial anisotropy [z being the easy axis and D negative in eq (1)], the correlation length, ξ, diverges exponentially at low temperatures as in the Ising model, and large oriented domains of 2ξ length along the chain are separated by narrow domain walls. In this situation, the susceptibility of the chain at low temperatures is given by the following relation:

$$\chi T/C \approx \exp(\Delta_\xi/k_B T) \quad (2)$$

where Δ_ξ is the energy to create a domain wall, C is the Curie constant per magnetic unit, and k_B is the Boltzmann constant. Therefore, when the magnetic anisotropy is uniaxial, a plot of the experimental data as $\ln(\chi T)$ vs $1/T$ gives a straight line with a slope directly related to Δ_ξ. Now the next question is, how can we express Δ_ξ as a function of the Hamiltonian parameters J and D? Indeed, the answer to this question in the general case is not so straightforward, but Barbara described two simple limits (Ising and Heisenberg) in 1973.[11] In this report, the shape and energy of the domain walls in 1D systems are discussed, and in particular in the Ising limit, i.e., as long as $|D/J|$ is larger than $^4/_3$, narrow domain walls (with single unit cell broadness) are expected with

$$\Delta_\xi = 4|J|S^2 \quad (3)$$

In the Heisenberg limit, i.e., when the anisotropy is small as $|D| \ll |J|$, a simple expression is obtained:

$$\Delta_\xi \approx 4S^2\sqrt{|JD|} \quad (4)$$

Between these two limits, the domain walls are spread on more than a unit cell and its creation energy, Δ_ξ, is a complex function of S, D, and J. This regime is still under investigation on a fundamental point of view, but it seems that it requires numerical approaches to link Δ_ξ, J, and D.[12]

II.2. Dynamics of the Magnetization: The Ising Limit. The description of the dynamics in these 1D systems is another, but more complicated, theoretical problem. The simplest way to describe the dynamics of magnetic chains relies on stochastic models.[13] In 1963, Glauber reported the first time-dependent statistics of an Ising chain using stochastic functions of time to model interacting spins in contact with a large thermal bath that spontaneously provokes spin flips.[2] Glauber's approach leads to an exponential decay of the magnetization and thus a single relaxation time (τ):

$$\tau = \frac{\tau_0}{1 - \tanh(\Delta_\xi/k_B T)} \quad (5)$$

where $\Delta_\xi = 4|J|S^2$ and τ_0 represents the characteristic flipping time for a magnetically isolated spin unit. In the low-temperature approximation and for ferromagnetic interactions along the chain, the relaxation time can be simplified as

$$\tau = \frac{\tau_0}{2}\exp(2\Delta_\xi/k_B T) \quad (6)$$

In Glauber's model, τ_0 is a simple adjustable parameter,[14] while indeed it is temperature-dependent in a more general case and especially when the theory is compared to the real magnetic data. In most of the experimental cases, the anisotropic Heisenberg model in the large anisotropy limit ($|D/J| > {}^4/_3$) has been used to describe the SCMs.[15] In this approach, τ_0 describes the characteristic flipping time of a single anisotropic spin inside a narrow domain wall, where it sees no local field. According to eq (1), the energy to reverse this spin is

$$\Delta_A = |D|S^2 \quad (7)$$

inducing that τ_0 also obeys an Arrhenius law:

$$\tau_0(T) = \tau_i \exp(\Delta_A/k_B T) \quad (8)$$

where τ_i is the characteristic time of the spin in contact with the thermal bath, in the absence of an energy barrier. When eq (8) is substituted in eq (6), the relaxation time of SCMs becomes

$$\tau(T) = \frac{\tau_i}{2}\exp[(2\Delta_\xi + \Delta_A)/k_B T] \quad (9)$$

The activated gap of this Arrhenius law is usually called $\Delta_{\tau 1}$ and thus

$$\Delta_{\tau 1} = 2\Delta_\xi + \Delta_A \quad (10)$$

This result is indeed very general because it depends only on the thermal dependence of the magnetic correlations. Therefore, eq (10) is verified for any Ising-like chain independently of the domain wall structure.[9] Considering narrow domain walls and single-ion anisotropy, eq (10) can be expressed as

$$\Delta_{\tau 1} = 8|J|S^2 + |D|S^2 \quad (11)$$

In all other cases (broad domain walls, complicated anisotropy, ...), the expression of $\Delta_{\tau 1}$, which is a function of the molecular parameters of the system (S, D, J, ...), is not straightforward.

II.3. Influence of the Defects. Because the correlation length grows very fast in 1D systems when the temperature decreases (i.e., ξ increases exponentially for the Ising or anisotropic Heisenberg models, vide supra), the presence of a very small number of defects along the chain strongly influences the static and dynamics properties of SCMs. Two types of approaches can be carried out depending on whether

(10) Loveluck, J. M.; Lovesey, S. W.; Aubry, S. *J. Phys. C: Solid State Phys.* **1975**, *8*, 3841.
(11) Barbara, B. *J. Phys. (Paris)* **1973**, *34*, 1039. and *J. Magn. Magn. Mater.* **1994**, *129*, 79. In these papers, our J and D parameters are noted W and K, respectively. .
(12) Vindigni, A.; Coulon, C. Private communications.
(13) For a review, see for example: Kawasaki, K. In *Phase Transitions and Critical Phenomena*; Domb, C., Green, M. S., Eds.; Academic Press: London, 1972; Vol. *2*, p 443.
(14) Suzuki, M.; Kubo, R. *J. Phys. Soc. Jpn.* **1968**, *24*, 51.
(15) Coulon, C.; Clérac, R.; Lecren, L.; Wernsdorfer, W.; Miyasaka, H. *Phys. Rev. B* **2004**, *69*, 132408.

the chain length, L, is considered as mono- or polydispersed. We will describe here only the monodispersed case, but the interested reader is addressed to ref 9 for the description of the polydispersed case. Imry and co-workers have described the magnetic susceptibility for a segment of n Ising spins[16] and have shown that a crossover temperature (T^*) exists when the correlation length is equal to L. Above T^*, a segment behaves as an infinite chain with an exponential regime [eq (2)], but at lower temperatures, all of the spins are parallel within the segment and can be reduced as an effective spin of size nS, inducing a Curie-like behavior with $\chi_n T/C \approx n$. The effect of defects (or a finite size of the chains) is also important on the dynamics of the SCMs especially. Luscombe et al. studied this problem in the frame of the Glauber model considering single spin flips.[17] As for the static susceptibility, a crossover is observed on the dynamics at T^* when $\xi \approx L$. For $T > T^*$, the dynamics of a segment of n Ising spins is the same as that for the infinite chain, and therefore eq (9) is valid. In the low-temperature regime, i.e., $T < T^*$, the flipping probability is much higher from the ends of the segment because these terminal spins are linked to only one neighbor and they have to overcome only one interaction to reverse. Hence, in this finite-size regime, the magnetic correlations still give a contribution to the relaxation time that can be expressed as

$$\tau_L(T) = \tau_i' \exp[(\Delta_\xi + \Delta_A)/k_B T] \quad (12)$$

The activated gap of this Arrhenius law is usually called $\Delta_{\tau 2}$, and thus

$$\Delta_{\tau 2} = \Delta_\xi + \Delta_A \quad (13)$$

As for eq (10), the relationship of eq (13) is also valid for an Ising-like chain with any domain wall structure even if the relationship between $\Delta_{\tau 2}$ and the molecular parameters of the system (S, D, J, ...) is not always easily determined. Considering narrow domain walls and single-ion anisotropy, eq (13) can be expressed as

$$\Delta_{\tau 2} = 4|J|S^2 + |D|S^2 \quad (14)$$

As summarized in this part of the paper, the magnetic susceptibility, i.e., static properties, and the dynamics, i.e., the magnetization relaxation, must be simultaneously analyzed to characterize unambiguously the SCM behavior. It appears for us that it is important to finish this theoretical paragraph by highlighting that eqs (2), (9), and (12) are very general to any Ising-like model independently of the domain wall broadness. In the case of narrow domain walls and single-ion anisotropy, the expressions of $\Delta_{\tau 1}$, $\Delta_{\tau 2}$, Δ_ξ, and Δ_A are simple functions of S, D, and J [eqs (3), (7), (11), and (14)], but in all other cases, analytical expressions are rarely available and this remains a subject of active research in order to model experimental results in this regime.[12]

III. Synthetic Strategies to SCMs

Considering the theoretical ingredients presented in section II, a simple design of SCMs could be achieved by connecting ferromagnetically Ising-type spins in one dimension. In this part of the Forum Article, several rational preparative routes toward SCMs are proposed. Section III.1 focuses on the use of SMMs as uniaxial anisotropic spin units to efficiently design SCMs. This approach also facilitates the understanding of SCM static and dynamic properties because they are built from SMMs with known intrinsic properties. In this section, two new zigzag chains that have the same formula as the known [Mn_2Ni] SCMs are presented to highlight the key role played by the magnetic anisotropy in balance with the intrachain interactions in the SCM dynamics. Section III.2 describes the synthetic strategy that consists of employing uniaxial anisotropic molecular units (which do not exhibit SMM properties themselves) that possess a well-defined Ising-type axis on their coordination sphere. As shown in section III.3, *metalloligands* containing various transition-metal ions have also been used to design SCM systems. The three first sections of this part III dedicated to the synthesis of SCM will try to answer the fundamental question, how can we rationally construct 1D SCM systems using various kinds of anisotropic metal ions? Finally, section III.4 presents several noteworthy SCM materials obtained serendipitously that could open a new way to design SCM systems.

III.1. Design of SCMs from SMMs. Following Glauber dynamics, Ising spins should be organized in a chain to obtain SCM properties. However, at the experimental level, only Ising-like spin sources are available. These precursors exhibit significant uniaxial magnetic anisotropy intrinsic to the metal ion and its ligand field. In this case and as presented in section II, an alternative anisotropic Heisenberg model is employed to describe the actual chains, i.e., quasi-Ising chains. Hence, it becomes very important to know the magnitude of (i) the anisotropic energy ($\Delta_A = |D|S^2$) of the building block and the intrachain correlation energy ($\Delta_\xi = 4|J|S^2$). Following these ideas, the groups of Miyasaka and Clérac have designed and studied simple 1D systems made of ferromagnetically coupled SMMs, which are well-known uniaxial anisotropic units possessing an intrinsic thermally activated relaxation time with an energy barrier of Δ_A. These systems exhibit SCM dynamics, and a quantitative analysis of the characteristic energies ($\Delta_{\tau 1}$, $\Delta_{\tau 2}$, Δ_ξ, and Δ_A) can be obtained in agreement with eqs (3), (7), (11), and (14).

The materials of general formula $[Mn^{III}_2(5\text{-Rsaltmen})_2\text{-}Ni^{II}(oxime)_2(L)_x]A_2$ [5-Rsaltmen^{2-} = *N*,*N*′-(1,1,2,2-tetramethylethylene)bis(5-Rsalicylideneiminate) with R = H and MeO; oxime = pyridine-2-aldoximate (pao), 1-methylimidazole-2-aldoximate (miao), and 1-ethylimidazole-2-aldoximate (eiao); L = monodentate N ligands such as pyridine, 4-picoline, 4-*tert*-butylpyridine, and *N*-methylimidazole with $x = 2$ or bidentate N ligands such as 2,2′-bipyridine and 1,10-phenanthroline with $x = 1$; $A^- = ClO_4^-$, BF_4^-, PF_6^-, ReO_4^-, and BPh_4^-] are built of chains of ferromagnetically coupled [Mn^{III}−ON−Ni^{II}−NO−Mn^{III}] $S = 3$ units (Figure 1).[5,18] In these systems, the ferromagnetic exchange is usually in the range of +0.4 to +0.9 K and the anisotropy parameter (D) of the spin unit is typically about −2.5 K. Therefore, these materials fall in the $|D/J| \gg {}^4/_3$ limit of Glauber dynamics. The anisotropic energy (Δ_A) of this [Mn_2Ni] unit

(16) Imry, Y.; Montano, P. A.; Hone, D. *Phys. Rev. B* **1975**, *12*, 253.
(17) Luscombe, J. H.; Luban, M.; Reynolds, J. P. *Phys. Rev. E* **1996**, *53*, 5852.

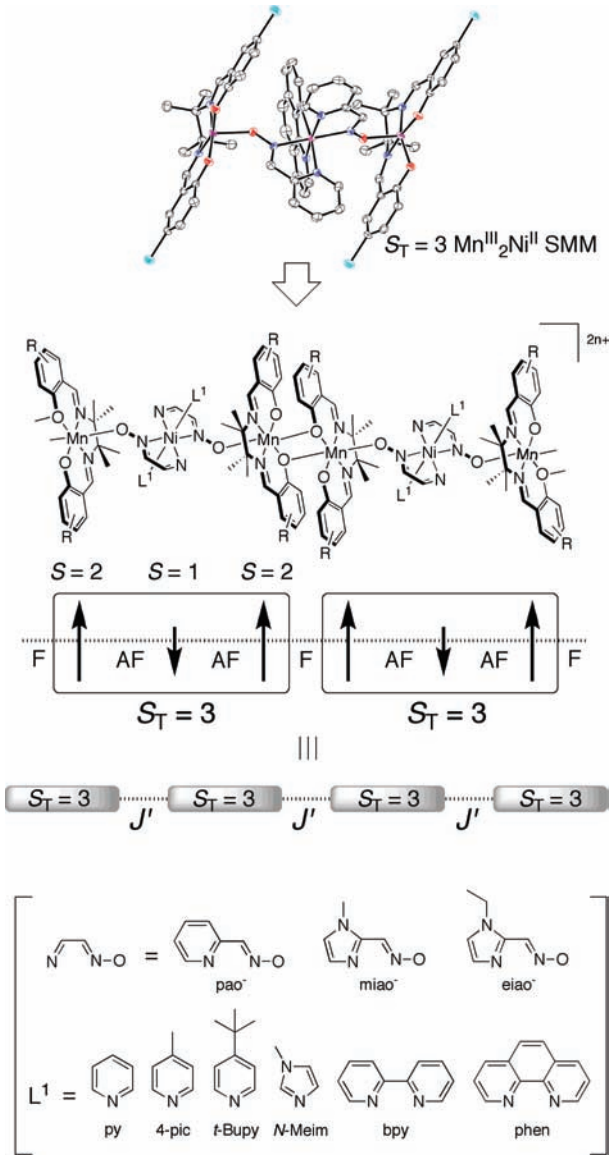

Figure 1. Route to the design of SCMs using an assembly of SMM units, in which the $[Mn^{III}_2Ni^{II}]$ SMM is, for example, $[Mn^{III}_2(5\text{-Clsaltmen})_2Ni^{II}(pao)_2(phen)](ClO_4)_2$ reported previously.[19]

is thus about 20 K, which has been confirmed by the analysis of the SMM behavior of isolated $[Mn^{III}-ON-Ni^{II}-NO-Mn^{III}]$ $S = 3$ units, $[Mn^{III}_2(5\text{-Rsaltmen})_2Ni^{II}(pao)_2(phen)](ClO_4)_2$ (R = Cl and Br).[19]

Figure 2 shows a plot of Δ_{eff} vs J in the family of $[Mn^{III}_2Ni^{II}]$ SCMs and SMMs.[18c] All data follow a linear trend and lead to the least-squares linear fit with $\Delta_{eff}/k_B = 22.4 + 64.4J/k_B$ (dashed line in Figure 2). The most important point is that this linear trend agrees with the expected correlation of the infinite-chain regime, $\Delta_{\tau 1} = \Delta_A + 2\Delta_\xi = |D|S^2 + 8JS^2$ or $\Delta_{\tau 1}/k_B = 21 + 72J/k_B$ (solid line in Figure 2). This result demonstrates that this family of materials exhibits the expected Glauber dynamics in the

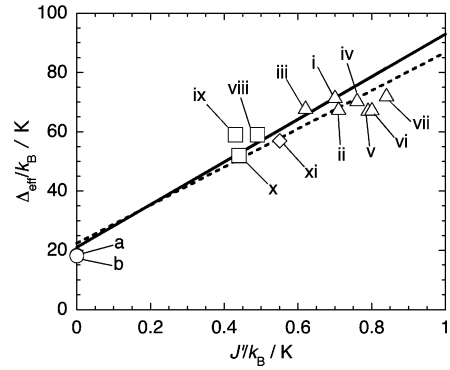

Figure 2. Plot of Δ_{eff} vs J' in the family of $[Mn^{III}_2Ni^{II}]$ regular SCMs (i−xi) and SMMs (a and b). The solid and dashed lines represent the expected line of $\Delta_{\tau 1}/k_B = 21 + 72J'/k_B$ based on the relationship of $\Delta_{\tau 1} = |D|S^2 + 8J'S^2$ with $|D|S^2/k_B = 21$ K from the data of a and b and the least-squares linear fit for all data ($\Delta_{eff}/k_B = 22.4 + 64.4J'/k_B$), respectively: (i) $[Mn_2(saltmen)_2Ni(pao)_2(py)_2](ClO_4)_2$; (ii) $[Mn_2(saltmen)_2Ni(pao)_2(4\text{-pic})_2](ClO_4)_2$ (4-pic = 4-picoline); (iii) $[Mn_2(saltmen)_2Ni(pao)_2(t\text{-Bupy})_2](ClO_4)_2$ (*t*-Bupy = 4-*tert*-butylpyridine); (iv) $[Mn_2(saltmen)_2Ni(pao)_2(N\text{-Meim})_2](ClO_4)_2$ (*N*-Meim = *N*-methylimidazole); (v) $[Mn_2(saltmen)_2Ni(pao)_2(py)_2](BF_4)_2$; (vi) $[Mn_2(saltmen)_2Ni(pao)_2(py)_2](PF_6)_2$; (vii) $[Mn_2(saltmen)_2Ni(pao)_2(py)_2](ReO_4)_2$; (viii) $[Mn_2(saltmen)_2Ni(miao)_2(py)_2](ClO_4)_2$ ($miao^-$ = 1-methylimidazole-2-aldoximate); (ix) $[Mn_2(saltmen)_2Ni(miao)_2(py)_2](PF_6)_2$; (x) $[Mn_2(saltmen)_2Ni(eiao)_2(py)_2](ClO_4)_2$ ($eiao^-$ = 1-ethylimidazole-2-aldoximate); (xi) $[Mn_2(saltmen)_2Ni(pao)_2(phen)](BPh_4)_2$; (a) $[Mn_2(5\text{-Clsaltmen})_2Ni(pao)_2(phen)](ClO_4)_2$; (b) $[Mn_2(5\text{-Brsaltmen})_2Ni(pao)_2(phen)](ClO_4)_2$.[18c]

$|D/J| \gg {}^4/_3$ limit and that the characteristic energies ($\Delta_{\tau 1}$, Δ_ξ, and Δ_A) are in agreement with eqs (3), (7), and (11).

Another representative example of a SMM-based SCM is the compound of formula $NEt_4[Mn^{III}_2(5\text{-MeOsalen})_2Fe^{III}(CN)_6]$ [5-MeOsalen^{2-} = *N*,*N*′-ethylenebis(5-methoxysalicylideneiminate)], which is composed of cyano-bridged linear-type $[Mn^{III}-NC-Fe^{III}-CN-Mn^{III}]$ SMM units with $S = {}^9/_2$.[20] The connection of the SMM units to form a chain is due to the formation of an out-of-plane dimer of $[Mn^{III}_2(5\text{-MeOsalen})_2]^{2+}$ as well as in the family of $[Mn^{III}_2Ni^{II}]$ SCMs (vide supra), consequently being a chain of ferromagnetically coupled $S = {}^9/_2$ SMMs. Single-crystal magnetization measurements at low temperatures demonstrated the Ising-type nature of the anisotropy. Large M vs H hysteresis curves were observed when the field was applied parallel to the chain direction (easy axis), and a linear dependence without hysteresis effects occurred when the field was applied perpendicular to the chain (hard plane). From static magnetic measurements, the values of the exchange coupling between the SMMs (J/k_B) and the anisotropic parameter of the SMM unit (D/k_B) were estimated as +0.07 and −0.94 K, respectively. Therefore, the derived values for the correlation ($\Delta_\xi = 4|J|S^2$) and anisotropic [$\Delta_A = |D|(S^2 - {}^1/_4)$] energies are 5.7 and 18.8 K, respectively. As expected, the dynamic magnetic measurements have revealed two kinds of relaxation regimes: infinite-chain ($\tau_{01} = 3.7 \times 10^{-10}$ s and $\Delta_{\tau 1}/k_B = 31$ K) and finite-chain ($\tau_{02} = 3 \times 10^{-8}$ s and $\Delta_{\tau 2}/k_B = 25$ K) regimes with a crossover temperature at 1.4 K. These energy barriers for the magnetization reversal can be well accounted by eqs (10) and (13) using Δ_ξ and Δ_A, indicating the presence of typical Glauber dynamics in this compound.

(18) (a) Miyasaka, H.; Clérac, R.; Mizushima, K.; Sugiura, K.; Yamashita, M.; Wernsdorfer, W.; Coulon, C. *Inorg. Chem.* **2003**, *42*, 8203. (b) Saitoh, A.; Miyasaka, H.; Yamashita, M.; Clérac, R. *J. Mater. Chem.* **2007**, *17*, 2002. (c) Miyasaka, H.; Saitoh, A.; Yamashita, M.; Clérac, R. *Dalton Trans.* **2008**, 2422.

(19) Miyasaka, H.; Nezu, T.; Sugimoto, K.; Sugiura, K.; Yamashita, M.; Clérac, R. *Chem.—Eur. J.* **2005**, *11*, 1592.

(20) Ferbinteanu, M.; Miyasaka, H.; Wernsdorfer, W.; Nakata, K.; Sugiura, K.; Yamashita, M.; Coulon, C.; Clérac, R. *J. Am. Chem. Soc.* **2005**, *127*, 3090.

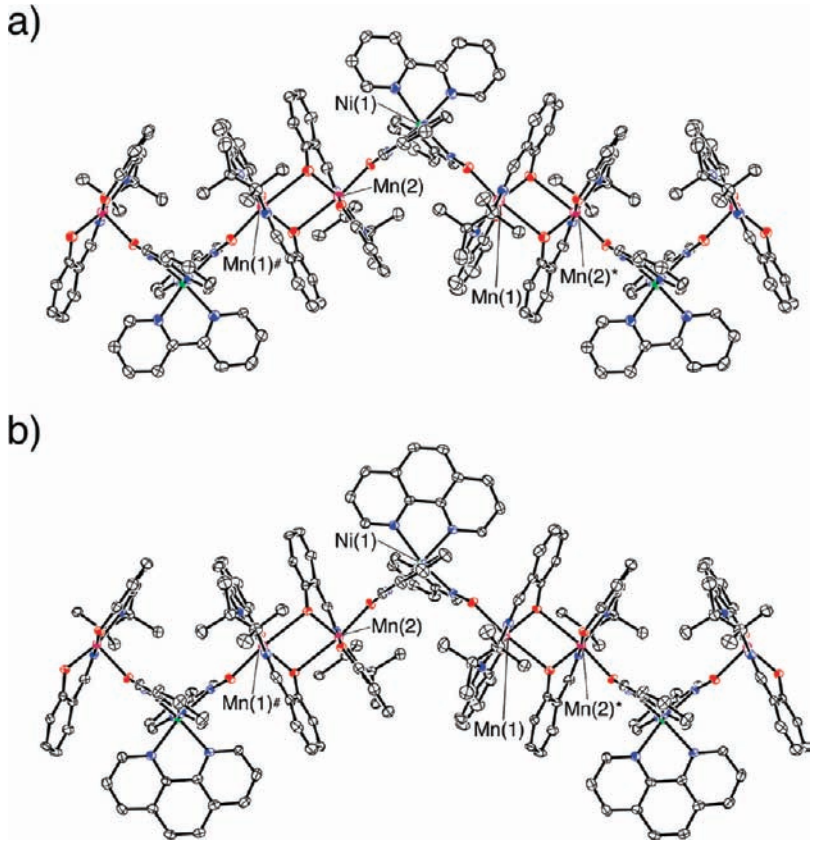

Figure 3. Chain motif of **1** (a) and **2** (b), where symmetry operations (* and #) are $x - {}^1/_2, -y + {}^1/_2, z - {}^1/_2$ and $x + {}^1/_2, -y + {}^1/_2, z + {}^1/_2$, respectively.

The most important point that should be mentioned here is that the dynamic behavior of the $S = {}^9/_2$ [Mn^{III}−NC−Fe^{III}−CN−Mn^{III}] SMM unit was confirmed by an isolated related compound, $NEt_4[Mn^{III}_2(salmen)_2(MeOH)_2Fe^{III}(CN)_6]$ [salmen^{2-} = *rac*-*N*,*N*′-(1-methylethylene)bis(salicylideneiminate)],[21] which exhibits SMM behavior explained using its intrinsic parameters: $S = {}^9/_2$ and $D/k_B = -1.25$ K ($\Delta_A/k_B = 25$ K).[20]

As shown by the two examples above, the combination between the correlation (Δ_ξ) and anisotropic (Δ_A) energies plays a critical role in achieving the SCM behavior based on the Glauber dynamics. Here, we take advantage of the present Forum Article to foresee the dependence of the SCM behavior on the anisotropic energy by introducing two new compounds: $[Mn^{III}_2(saltmen)_2Ni^{II}(pao)_2(L)](PF_6)_2$ with L = bpy (**1**) and phen (**2**). Considering the series of $[Mn^{III}_2Ni^{II}]$ SCMs (Figure 1), these two systems have a similar bridging motif, which consists of [−Mn^{III}−ON−Ni^{II}−NO−Mn^{III}−$(O_{Ph})_2$−] motifs, but a zigzag $[Mn^{III}_2Ni^{II}]$ chain is observed as a result of the NO-*cis*-coordination mode of the [$Ni(pao)_2(L)$] moiety that "bent" the [Mn−Ni−Mn] trinuclear $S = 3$ unit. Consequently, these compounds do not exhibit SCM behavior at temperatures above 1.8 K. It is very interesting to analyze the reason for the change of magnetic properties that contrast with the linear-type compounds. The chain motifs of **1** and **2** are depicted in Figure 3, and the packing features of **2** are given in Figure 4. Except for the geometry around the Ni^{II} ion, the bridging feature is analogous to the one for $[Mn^{III}_2Ni^{II}]$ SCMs. Because of the crystal symmetry of **1** and **2**, the $[Mn^{III}_2Ni^{II}]$ units exhibit two kinds of Mn−Ni bonds, Mn(1)−Ni(1) and Mn(2)−Ni(1), but only one Mn···Mn bridging mode: Mn(1)−$(O_{Ph})_2$−Mn(2). It should be noted that the values of the Mn−O_{Ph}* distance (a parameter that strongly affects the exchange interaction between Mn^{III} ions, i.e., the exchange interaction between the $S = 3$ unit spins) are 2.689(4) Å [Mn(1)−O(5)*] and 2.714(4) Å [Mn(2)−O(1)*] for **1** and 2.5911(18) Å [Mn(1)−O(5)*] and 2.6202(19) Å [Mn(2)−O(1)*] for **2**. They are somewhat longer than those of the $[Mn^{III}_2Ni^{II}]$ SCM family.[5,18] As shown Figure 4, the chains run along the $a + c$ direction and the nearest interchain M···M distance corresponds to Mn(1)···Ni(1) separation with values of 9.46 (**1**) and 9.81 Å (**2**).

Figure 5 shows the χT vs T plots of **1** and **2** and their fitting curves in the temperature range above 30 K using a conventional linear trinuclear Heisenberg model with $S = (2, 1, 2)$ and taking into account the interunit interaction (zJ') in the frame of the mean-field approximation ($z = 2$ assumed as an intrachain interaction).[5] The best-fit parameters are $g = 1.96$, $J/k_B = -22.8$ K, and $J'/k_B = 0.16$ K for **1** and $g = 1.95$, $J/k_B = -22.6$ K, and $J'/k_B = 0.32$ K for **2**. The J value in both compounds indicates that the [Mn^{III}−ON−Ni^{II}−NO−Mn^{III}] bent unit possesses an $S = 3$ ground state at low temperatures ($T < 10$ K) as well as the linear unit of the $[Mn^{III}_2Ni^{II}]$ SCMs. The J' value of **1** is smaller than that of **2**, reflecting the somewhat greater value of the Mn−O* bond

(21) Miyasaka, H.; Ieda, H.; Matsumoto, N.; Re, N.; Crescenzi, R.; Floriani, C. *Inorg. Chem.* **1998**, *37*, 25.

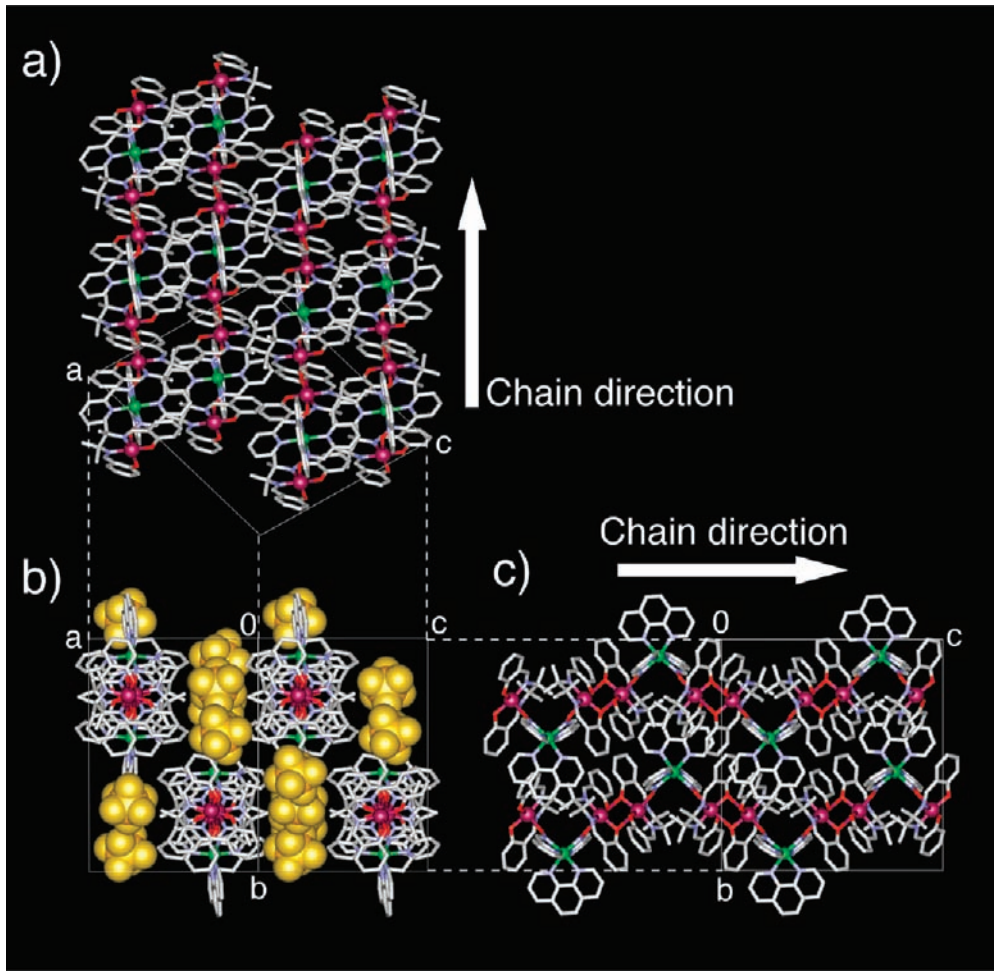

Figure 4. Packing diagrams of **2**, where parts a−c are projection views along the *b* axis, the $a + c$ direction, and the *a* axis, respectively. The PF_6^- counteranions as CPK representations are only displayed in part b.

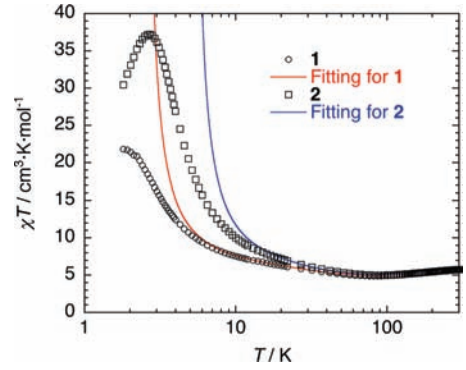

Figure 5. χT vs *T* plot for **1** (circle) and **2** (square), where the red and blue lines represent simulation curves done in the temperature range of 30−300 K (see the text).

distance in **1**. Although the exchange coupling J' between the $S = 3$ units is relatively small, if the anisotropic energy was identical with that of the $[Mn^{III}_2Ni^{II}]$ SCM family ($\Delta_A/k_B \approx 22$ K), **1** and **2** should be SCMs and should follow the relationship of Figure 2. *This is experimentally not the case*, and therefore the origin of the striking difference between the magnetic properties of the $[Mn^{III}_2Ni^{II}]$ SCMs and these two compounds are necessarily the result of a weakening of the magnetic anisotropy brought by the bent $S = 3$ units.

Figure 6a shows the angular dependence (with *b* and $a + c$ being the rotation axes) of the normalized magnetization measured at 2 K under an applied direct current (dc) field of 5 kOe using an oriented single crystal of **2**. A strong magnetic anisotropy is observed, but the presence of an intermediate magnetic axis is clearly observed here while it was lacking in the original $[Mn^{III}_2Ni^{II}]$ SCM, $[Mn^{III}_2(saltmen)_2Ni^{II}(pao)_2(py)_2](ClO_4)_2$ (in such a compound, a uniaxial symmetry was observed, i.e., an easy axis and a hard plane).[5,15,18a] As seen on the rotation figure around the *b* axis (that is, by symmetry, a magnetic axis in a monoclinic space group), the $a + c$ direction (corresponding to the chain direction) is as expected the easy magnetic axis (noted *i* in Figure 6), whereas a perpendicular axis to the (−101) plane (the $-a + c$ direction) is the hard magnetic axis (noted *ii* in Figure 6). Meanwhile, the rotation pattern around the $a + c$ axis (chain direction) confirms the positions of the hard and intermediate (noted *iii* in Figure 6) magnetic axes along the $-a + c$ and *b* directions. The field dependence of the magnetization measured along the three principal directions at 2 K is shown in Figure 6b. With increasing fields, the easy-axis magnetization increases steeply at very low fields to saturate above 1 T, whereas in the hard direction, the magnetization increases linearly up to around 4.5 T and gradually to 7 T (even at 7 T, the magnetization is not saturated with $M/M_s \approx 0.9$), as is typically observed for the hard-axis behavior. The magnetization in the intermediate *b*

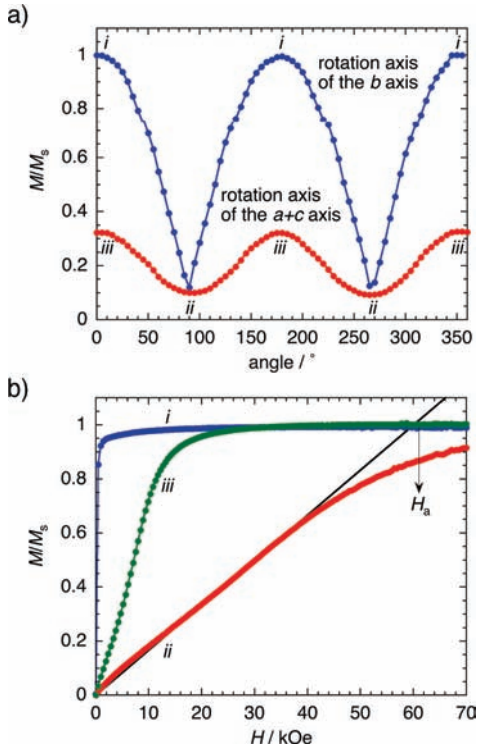

Figure 6. Variation of the magnetization of **2** as a function of the single-crystal rotation angle (a) and field (b). In part a, the blue and red plots were measured as a rotation axis corresponding to the *b* crystal axis and the $a + c$ axis, respectively. The *MH* curves of i (easy axis), ii (hard-axis), and iii (middle axis) in part b were measured at distinct angles determined in part a. The solid black line of part b represents the least-squares linear fit of the hard-axis magnetization in the range of 0−4 T and defines the anisotropic field H_a at the crossing point with $M_s = 1$.

axis increases more easily than the one on the hard axis but still linearly up to an inflection point at around 7 kOe, followed by a gradual increase to M_s. The presence of the intermediate axis implies the loss of uniaxial anisotropy of this system. Nevertheless, the anisotropy field H_a can be roughly estimated from the hard-axis magnetization behavior by $H_a \approx 2|D|S_T/g\mu_B$. The extrapolation of the linear increasing region of the hard-axis magnetization to $M/M_s = 1$ was used to determine H_a to about 6.1 T (solid black line in Figure 6b), which leads to $D/k_B = -1.33$ K (as $g = 1.95$) and, thus, $\Delta_A/k_B = 12.0$ K. These values are approximately half of the magnitude of $[Mn^{III}_2Ni^{II}]$ SCMs ($D/k_B \approx -2.5$ K and $\Delta_A/k_B = 22.5$ K).[5,18] This result points out the decisive role of anisotropy and why the present zigzag chains do not exhibit SCM behavior above 1.8 K, as is observed in the linear-type $[Mn^{III}_2Ni^{II}]$ chains. Hence, these compounds highlight experimentally the importance of the intrachain magnetic interactions and particularly the crucial role of the magnetic anisotropy of the chain unit to design new SCM compounds.

To conclude this paragraph, it should be mentioned that 1D arrangements of SMMs are also reported in a regime where the inter-SMM interactions along chain can be simply considered as a perturbation from the intrinsic behavior of the SMM units.[22−25] Such materials might be considered as intermediate between SMM and SCM systems.[24] For example, Clérac and co-workers demonstrated such a behavior in a hydrogen-bonded 1D compound of $[Mn^{III}_2]$ SMM units ($[Mn^{III}_2(salpn)_2(H_2O)_2][ClO_4]_2$ [salpn^{2-} = *N*,*N*′-propanediaminebis(salycilideneiminate)],[24] and Christou et al. showed the influence of the inter-SMM interactions in a $[Mn_7]$ SMM ($[Mn_7O_8(O_2SePh)_8(O_2CMe)(H_2O)]$) organized in one dimension thanks to weak Se···O contacts.[25]

III.2. Design of SCMs Using Uniaxial Anisotropic Complexes. Although we are fully aware of the availability of SMM units for the design of SCMs (see section III.1), the choice of SMMs that have concomitant coordination sites capable of assembling with other bridging groups without significant structural change is, in practice, not easy at all. Indeed, except for the $[Mn^{III}_2Ni^{II}]$ and $[Mn^{III}_2Fe^{III}(CN)_6]$ SMM units, only one kind of SMM, a double-cuboidal $[Mn^{II}_2Mn^{III}_2]$ SMM, has been employed for the design of SMM-based materials so far.[26] An alternative method to synthesize SCMs is to use uniaxial anisotropic complexes, even if they are not SMMs. For example, complexes based on octahedral Co^{II}, Mn^{III}, or Ln^{III} metal ions, exhibiting uniaxial anisotropy and available coordination sites, have been used as precursors to the design of SCM systems. The organization of such complexes in a heterospin 1D array with paramagnetic bridging ligands (e.g., metal complexes and organic radicals) is expected to yield chains with either ferromagnetic or ferrimagnetic arrangements. This rational synthetic strategy to the design of SCMs opens a wide diversity of systems with possible SCM properties. However, we have to notice that, for these types of alternating heterospin systems, there is for the moment no analytical expression of the main characteristic energies ($\Delta_{\tau 1}$ and $\Delta_{\tau 2}$) in relation to the *S*, *D*, and *J* parameters. Therefore, a detailed analysis of these systems remains difficult, in contrast to simple homospin systems described in section II. This is one of the future theoretical issues that will have to be tackled in this field of research.

The six-coordinated, high-spin, cobalt(II) complexes can possess an effective spin of $S_{eff} = {}^1/_2$ with a strong Ising character owing to strong spin−orbit coupling. Therefore, the spin of the Co^{II} metal ion can be regarded as a quantum Ising-type spin. The first example of SCMs, $[Co^{II}(hfac)_2$-(NITPhOMe)] (hfac = hexafluoroacetylacetonate; NITPhOMe = 4′-methoxyphenyl-4,4,5,5-tetramethylimidazoline-1-oxyl-3-oxide), provided by Gatteschi et al. in 2001 has thus been designed using this anisotropic spin where the $[Co^{II}(hfac)_2]$ unit was chosen as an Ising-type building block.[4]

(22) (a) Wernsdorfer, W.; Aliaga-Alcalde, N.; Hendrickson, D. N.; Christou, G. *Nature* **2002**, *416*, 406. (b) Tiron, R.; Wernsdorfer, W.; Foguet-Albiol, D.; Aliaga-Alcalde, N.; Christou, G. *Phys. Rev. Lett.* **2003**, *91*, 227203. (c) Tiron, R.; Wernsdorfer, W.; Aliaga-Alcalde, N.; Christou, G. *Phys. Rev. B* **2003**, *68*, 140407.
(23) Yoo, J.; Wernsdorfer, W.; Yang, E.-C.; Nakano, M.; Rheingold, A. L.; Hendrickson, D. N. *Inorg. Chem.* **2005**, *44*, 3377.
(24) Lecren, L.; Wernsdorfer, W.; Li, Y.-G.; Vindigni, A.; Miyasaka, H.; Clérac, R. *J. Am. Chem. Soc.* **2007**, *129*, 5045.
(25) Chakov, N. E.; Wernsdorfer, W.; Abboud, K. A.; Christou, G. *Inorg. Chem.* **2004**, *43*, 5919.
(26) (a) Lecren, L.; Roubeau, O.; Coulon, C.; Li, Y.-G.; Le Goff, X. F.; Wernsdorfer, W.; Miyasaka, H.; Clérac, R. *J. Am. Chem. Soc.* **2005**, *127*, 17353. (b) Lecren, L.; Roubeau, O.; Li, Y.-G.; Le Goff, X. F.; Miyasaka, H.; Richard, F.; Wernsdorfer, W.; Coulon, C.; Clérac, R. *Dalton Trans.* **2008**, 755. (c) Roubeau, O.; Clérac, R. *Eur. J. Inorg. Chem.* **2008**, 4325.

Importantly, the favorable anisotropic nature around the Co^{II} ion in this coordination environment has indeed been proven in the mononuclear complex $[Co^{II}(hfac)_2(NITPhOMe)_2]$.[27]

In six-coordinated manganese(III) complexes, the anisotropic axis and available coordination sites are codirected out of the plane of the partially blocking polydentate ligands (most likely fully deprotonated Schiff base and porphyrinate tetradentate type ligands), corresponding to the Jahn−Teller axis. In such cases, chains assembled with coordination-donor building blocks or building organic/inorganic groups are able to have an easy axis of the magnetization. A simple case following the Glauber dynamics is given by the $[Mn^{III}(TPP)O_2PHPh]\cdot H_2O$ (TPP^{2-} = *meso*-tetraphenylporphyrinate and O_2PHPh^- = phenylphosphinate) system reported by Sessoli and co-workers.[28] This compound is a zigzag 1D compound that behaves as a chain of canted antiferromagnetically coupled Mn^{III} $S = 2$ spins with $D_{Mn}/k_B = -4.7(2)$ K, $J/k_B = -0.68(4)$ K, and $\theta = 34.6°$ and that exhibits a thermally activated relaxation time with $\Delta_{\tau 1}/k_B = 36.8$ K (for a polycrystalline sample). Because of $|D/J| \gg {}^4/_3$, this energy barrier for the magnetization reversal has been simply interpreted by $\Delta_{\tau 1}/k_B = 8|J|S^2 \cos\theta/k_B + |D|S^2/k_B \approx 37(2)$ K, in good agreement with the experimental value. Another representative example using manganese(III) complexes is a class of alternating chains composed of manganese(III) complexes with Schiff base or porphyrin ligands[29] and TCNQ or TCNE radicals, which are regular alternating chains of antiferromagnetically coupled $S = 2$ and ${}^1/_2$ spins. Their SCM behavior was first shown in $[Mn^{III}(5\text{-TMAM-saltmen})(TCNQ)](ClO_4)_2$ [5-TMAMsaltmen = *N*,*N*′-1,1,2,2-tetramethylethylenebis(5-trimethylammoniomethylsalicylideneiminate)].[30] In this chain, the spin units of the Mn^{III} ion ($S = 2$) and $TCNQ^{\bullet -}$ ($S = {}^1/_2$) are strongly antiferromagnetically coupled ($J/k_B = -96$ K) and they align to the chain direction because of strong anisotropy ($D_{Mn}/k_B = -2.4$ K) induced by the Mn^{III} ion. As expected from this situation, observed relaxation dynamics of the magnetization was assigned to SCM behavior with $\Delta_{\tau 1}/k_B = 94.1$ K (infinite chain regime) and $\Delta_{\tau 2}/k_B = 67.7$ K (finite chain regime) with a crossover temperature of 4.5 K. The Δ_ξ value estimated from a $\ln(\chi' T)$ vs T plot is 26.5 K, in good agreement with the value of $(\Delta_{\tau 1} - \Delta_{\tau 2})/k_B = 26.4$ K. Nevertheless, this SCM behavior cannot be fully explained by the Glauber dynamics because this system does not fall in the Ising limit with $|D/J| < {}^4/_3$. In this case, eqs (3), (11), and (14) are not valid, and in the frame of the available theory on SCM, it is not possible to relate the magnetic parameters (*S*, *J*, and *D*) with the characteristic energy gaps.

Lanthanide(III) complexes containing terbium, dysprosium, holmium, or erbium are other interesting precursors available as anisotropic building blocks to design SCMs. In 2005, Gatteschi et al. have reported the occurrence of SCM behavior in alternating chains of $[Ln(hfac)_3]$ and a nitronyl nitroxide radical.[31] One problem in such compounds with lanthanide complexes is the fact that the design (and evaluation) of the anisotropic nature of chains (magnitude and direction) becomes problematic because of the anisotropic nature of lanthanide complexes that changes dramatically with the geometry of their coordination polyhedron and the types of surrounding ligands. Both factors make it difficult to find their easy-axis position and therefore to analyze in detail the obtained magnetic properties.

As illustrated here, the molecular assembly of well-defined *anisotropic building blocks* (i.e., uniaxial anisotropic units) like octahedral cobalt(II) and manganese(III) Schiff bases, manganese(III) porphyrinate, or lanthanide(III) complexes is one of the most rational methods to obtain SCM systems. The next paragraph introduces another synthetic route to SCMs by using isotropic paramagnetic building blocks (named hereafter as metalloligands), which are able to act as ligands to catch anisotropic metal ions needed to obtain SCM behavior.

III.3. Metalloligand Approach to SCMs. In sections III.1 and III.2, we discussed the design of SCMs using SMMs and uniaxial anisotropic complexes as elementary units that can rationally add the anisotropic nature into the resulting chain assemblies. The introduced building blocks could be assembled in one direction, choosing, for example, linear-type bridging ligands. A priori this is not an easy task because of the required functionalization of the precursor and the unpredictable structural changes that it may undergo in the polymerization process, as noticed in the zigzag chains of $[Mn^{III}_2Ni^{II}]$ (see section III.1). These difficulties can be overcome with careful tailoring of the building block that will act as a paramagnetic bridging ligand. This is illustrated hereafter by two rational synthetic routes toward SCMs that are based on the use of the complex-as-ligand strategy, with the metalloligands (Lewis bases) being stable cyano- and oxamato-bearing metal complexes capable of coordinating to anisotropic metal ions (Lewis acids).

III.3.1. Cyano-Bridged SCMs. Most of the cyanide-based molecular materials have been prepared by using quite stable hexacyanometallate complexes of formula $[M(CN)_6]^{(6-m)-}$ as ligands toward either fully solvated or partially blocked metal ions.[32,33] The well-known Prussian Blue analogues and a great variety of multidimensional bimetallic assemblies extended through M−C−N−M′−N−C− linkages were obtained through this synthetic route. In an attempt to extend the vast cyanide chemistry to the low-dimensional-

(27) Caneschi, A.; Gatteschi, D.; Lalioti, N.; Sessoli, R.; Sorace, L.; Tangoulis, V.; Vindigni, A. *Chem.—Eur. J.* **2002**, *8*, 286.
(28) Bernot, K.; Luzon, J.; Sessoli, R.; Vindigni, A.; Thion, J.; Richeter, S.; Leclercq, D.; Larionova, J.; van der Lee, A. *J. Am. Chem. Soc.* **2008**, *130*, 1619.
(29) Miller, J. S. *Inorg. Chem.* **2000**, *39*, 4392, and references cited therein. .
(30) Miyasaka, H.; Madanbashi, T.; Sugimoto, K.; Nakazawa, Y.; Wernsdorfer, W.; Sugiura, K.; Yamashita, M.; Coulon, C.; Clérac, R. *Chem.—Eur. J.* **2006**, *12*, 7028.
(31) (a) Bogani, L.; Sangregorio, C.; Sessoli, R.; Gatteschi, D. *Angew. Chem., Int. Ed.* **2005**, *44*, 5817. (b) Bernot, K.; Bogani, L.; Caneschi, A.; Gatteschi, D.; Sessoli, R. *J. Am. Chem. Soc.* **2006**, *128*, 7947.
(32) Dunbar, K. R.; Heintz, R. A. *Prog. Inorg. Chem.* **1997**, *45*, 1023.
(33) (a) Verdaguer, M.; Bleuzen, A.; Marvaud, V.; Vaissermann, J.; Seuleiman, M.; Desplanches, C.; Scuiller, A.; Train, C.; Garde, R.; Gelly, G.; Lomenech, C.; Rosenman, I.; Veillet, P.; Cartier, C.; Villain, F. *Coord. Chem. Rev.* **1999**, *190−192*, 1023. (b) Ohba, M.; Okawa, H. *Coord. Chem. Rev.* **2000**, *198*, 313. (c) Tanase, S.; Reedijk, J. *Coord. Chem. Rev.* **2006**, *250*, 1501. (d) Miyasaka, H.; Saitoh, A.; Abe, S. *Coord. Chem. Rev.* **2007**, *251*, 2622.

Scheme 1

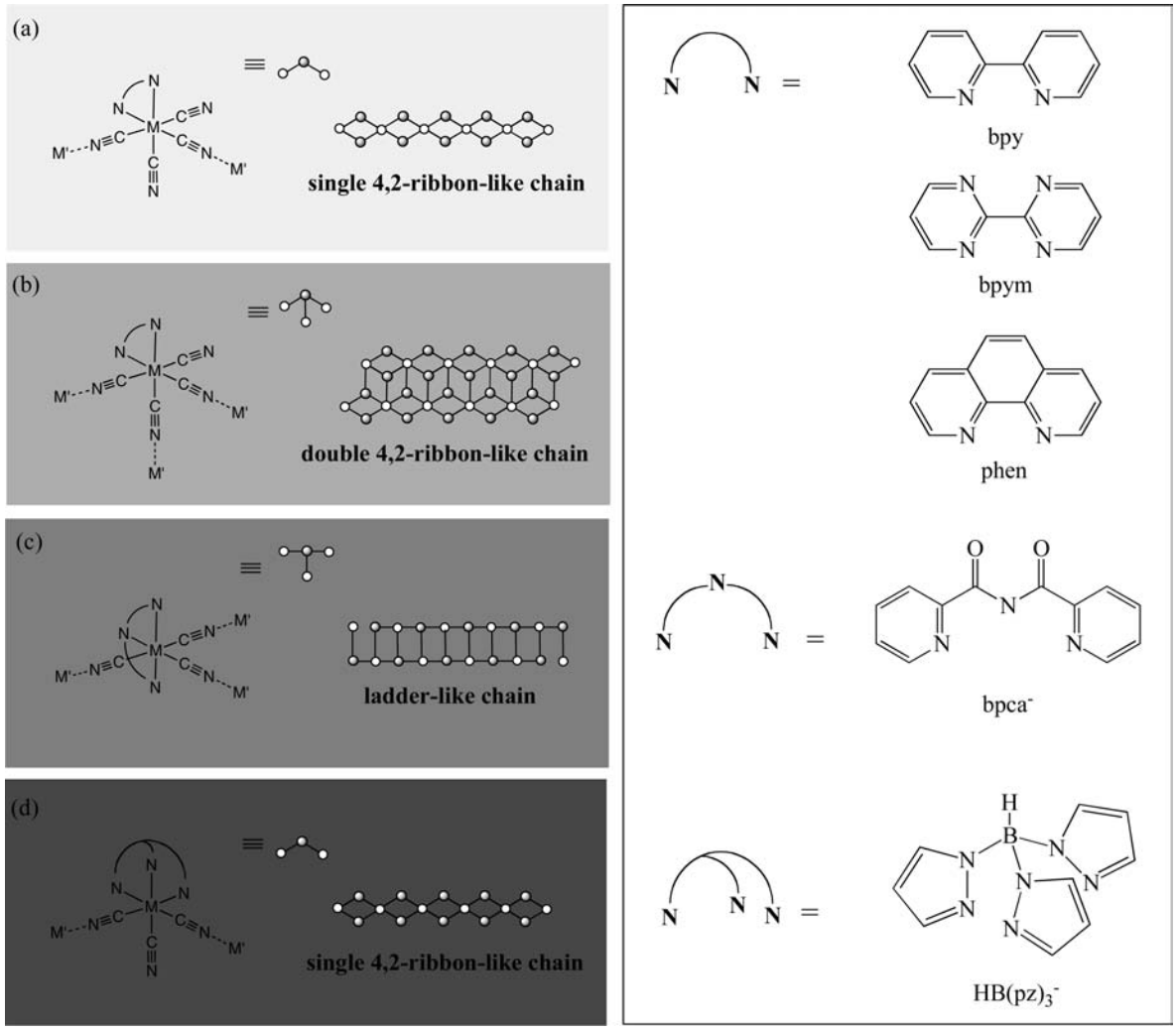

ity regime, an alternative synthetic route was developed where the hexacyanometallate unit is replaced by the stable six-coordinate complexes of the general formula $[M(L)(CN)_x]^{(x+1-m)-}$ (M = paramagnetic transition-metal ion and L = polydentate ligand).[34] The versatility and richness of this building block as a ligand is well illustrated by the number of parameters on which the synthetic chemist can play: (i) the spin value and anisotropy of M, which depend on the electronic configuration of the metal ion; (ii) the charge of the cyano-bearing unit, which will depend on the oxidation state of M and the charge of L, and its denticity, which determines the number of cyano ligands (four or three when L is a bidentate or tridentate group); (iii) the denticity of L also fixes the stereochemistry (for instance, *mer* or *fac* arrangements when L = tridentate ligand); (iv) the role of L not only is that of a blocking ligand but also can exert additional functions: to act as a bridge [in the case of L = 2,2′-bipyrimidine (bpym)] or to be involved in supramolecular interactions [$\pi-\pi$ interactions in the case of α-diimines such as 2,2′-bipyridine (bpy) or 1,10-phenanthroline (phen)] or hydrogen bonding [in the case of L = hydrotris(1-pyrazolyl)borate ($HB(pz)_3^-$)], with other possibilities such as redox activivity, photosensitivity, or chirality also being considered.

The use of $[M(L)(CN)_x]^{(x+1-m)-}$ as a ligand toward fully solvated metal ions has provided a great variety of discrete heterometallic species[35] as well as 1D compounds (Scheme 1).[35d,e,36] Some of these chains exhibit slow relaxation of the magnetization and hysteresis effects, typical features of SCMs.[36b−f,k−m] We will focus hereafter on two of them, namely, the Ising-like systems $\{[Fe^{III}(bpy)(CN)_4]_2Co^{II}(H_2O)_2\}\cdot 4H_2O$[36b] and $\{[Fe^{III}(bpym)(CN)_4]_2Co^{II}(H_2O)_2\}\cdot 6H_2O$[36e] because of their magnetostructural relevance.

These two compounds are neutral 4,2-ribbon-like bimetallic chains (Scheme 1a), where the low-spin iron(III) precursor exhibits a bridging bis-monodentate coordination mode through two of its four cyano groups in *cis* positions toward two *trans*-diaquacobalt(II) units. The intrachain magnetic coupling between the low-spin Fe^{III} and the high-spin Co^{II} ions is ferromagnetic in the two examples. The chains in the bpy compound run parallel to the crystallographic *a* axis, and they are very well isolated from each other. They exhibit the typical signature of a SCM with values of $\tau_0 = 9.4 \times$

(34) Lescouëzec, R.; Toma, L. M.; Vaissermann, J.; Verdaguer, M.; Delgado, F. S.; Ruiz-Pérez, C.; Lloret, F.; Julve, M. *Coord. Chem. Rev.* **2005**, *249*, 2691.

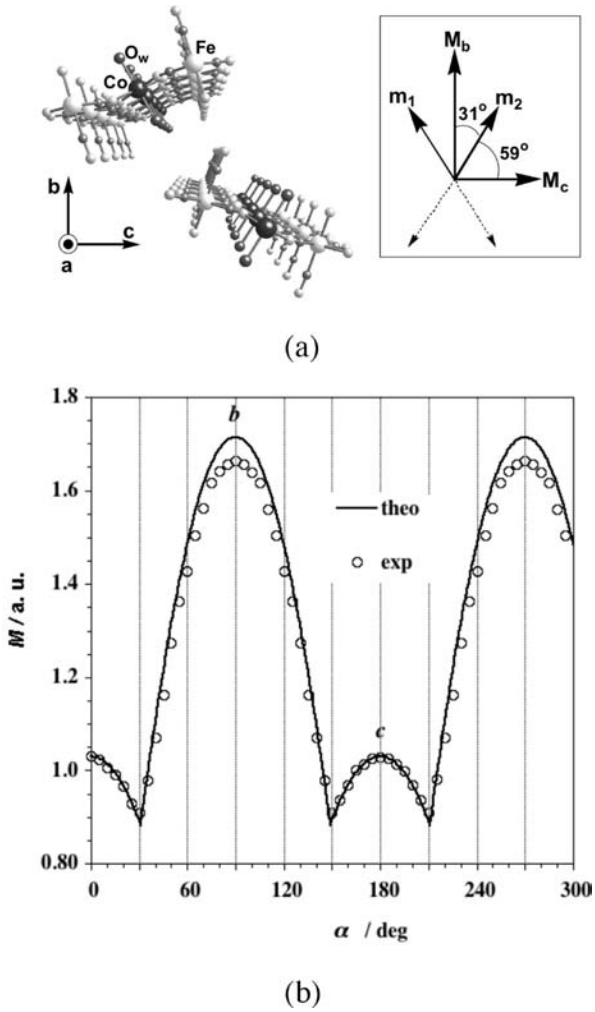

Figure 7. (a) Orientation of the magnetization local orientations in $\{[Fe^{III}(bpy)(CN)_4]_2Co^{II}(H_2O)_2\}\cdot 4H_2O$. (b) Dependence of the magnetization (arbitrary units) of a single crystal vs the rotation angle α in the *bc* plane under an applied magnetic field of 0.5 T at 5.0 K. The values of 0 and 90° correspond to *H*∥*c* and *H*∥*b*, respectively: (○) experimental data; (—) theoretical curve through simple vector calculations. Reproduced with permission of ref 36b. Copyright Wiley-VCH Verlag GmbH & Co. KGaA.

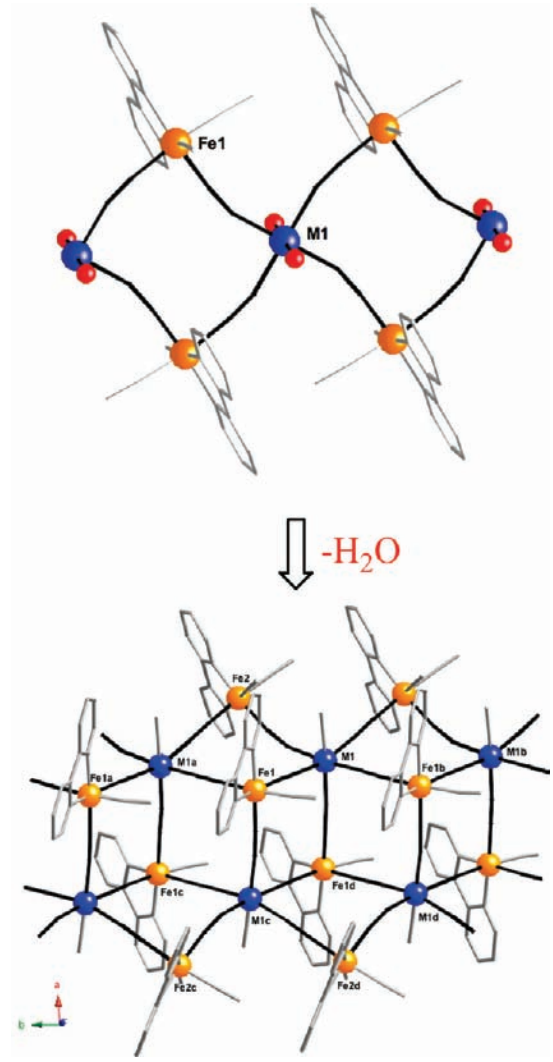

Figure 8. Schematic drawing showing the condensation of two $\{[Fe^{III}(bpy)(CN)_4]_2M^{II}(H_2O)_2\}\cdot 4H_2O$ chains to afford the double 4,2-ribbon-like motif (M = Co or Mn).[36c]

10^{-12} s and $\Delta_\tau/k_B = 142$ K. One of the peculiarities of this compound is the occurrence of two different orientations of the chains in the unit cell with the easy magnetic axes defined by the $Co-O_w$ bonds, which are located in the *bc* plane (Figure 7a). This knowledge allowed us to reproduce theoretically the temperature dependence of the magnetization on oriented single crystals in the *bc* plane (Figure 7b).

Another relevant feature associated with this compound is its transformation into a double 4,2-ribbon-like chain of formula $\{[Fe^{III}(bpy)(CN)_4]_2M^{II}(H_2O)\}\cdot MeCN\cdot {}^1/_2H_2O$[36c] (M = Co and Mn; Scheme 1b and Figure 8) when the reaction between the precursor $[Fe(bpy)(CN)_4]^-$ and the fully solvated M^{II} ions is carried out in a 90:10 (v/v) $MeCN/H_2O$ mixture. There are two types of $[Fe(bpy)(CN)_4]^-$ bridging units [Fe(1) and Fe(2)] in this double chain: Fe(1) acts as a bis-monodentate coordination mode through two *cis*-cyanide ligands, whereas Fe(2) adopts a tris-monodentate mode through three *fac*-cyanide groups. The magnetic properties of the double chain for M = Co are those of ferromagnetically coupled $[Fe^{III}_2Co^{II}]$ chains with a weak interchain antiferromagnetic coupling resulting in metamagnetic behavior. The value of the critical field (H_c) to overcome the interchain antiferromagnetic interaction is of only $H_c = 600$ Oe. The magnetic behavior of the compound $\{[Fe^{III}(bpy)(CN)_4]_2Co^{II}(H_2O)\}\cdot MeCN\cdot {}^1/_2H_2O$ under a dc field $H > 600$ Oe is like that of the ferromagnetic chain $\{[Fe^{III}(bpy)(CN)_4]_2Co^{II}(H_2O)_2\}\cdot 4H_2O$,[36b] providing thus an unprecedented example of a double SCM.

As far as the bpym-containing $[Fe^{III}_2Co^{II}]$ chain is concerned, its structure consists of neutral cyanide-bridged 4,2-ribbon-like bimetallic chains running parallel to the crystallographic *a* axis. Curiously, these chains are stacked along the *b* axis through hydrogen bonds involving centrosymmetric water hexameric rings with two dangling water molecules in *trans* positions to form a layered structure (Figure 9a).[36e] It deserves to be noted that the main structural difference with the related bpym-containing $[Fe^{III}_2Cu^{II}]$ chain $\{[Fe^{III}(bpym)(CN)_4]_2Cu^{II}(H_2O)_2\}\cdot 6H_2O$ is the occurrence in this last compound of an original motif of fused four- and five-membered water rings that interlink the neutral chains to afford also a supramolecular layered structure (Figure 9b). In both compounds, the chains are ferromagnetically coupled,

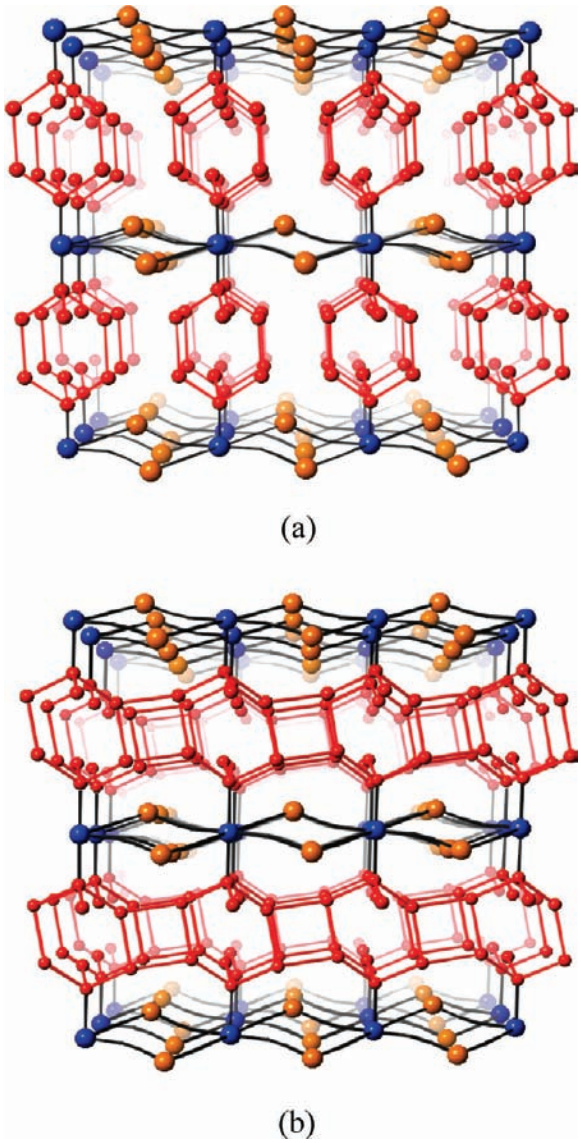

Figure 9. (a) Projection down the *c* axis showing the layered structure of $\{[Fe^{III}(bpym)(CN)_4]_2Co^{II}(H_2O)_2\}\cdot 6H_2O$. The bpym and terminal cyanide ligands have been omitted for clarity. (b) Projection down the *c* axis showing the layered structure of $\{[Fe^{III}(bpym)(CN)_4]_2Cu^{II}(H_2O)_2\}\cdot 6H_2O$. The red color has been used to visualize the water molecules and the network of hydrogen bonds.[36e]

with the $[Fe^{III}_2Cu^{II}]$ one being an example of strict orthogonality between the two interacting magnetic orbitals, t_{2g} (at the low-spin Fe^{III}) vs e_g (at the Cu^{II}) with weak interchain antiferromagnetic interactions (the values of H_c being 160 and 400 Oe for $[Fe^{III}_2Co^{II}]$ and $[Fe^{III}_2Cu^{II}]$, respectively). Most likely, the water motifs interlinking the chains provide the exchange pathway for the weak interchain antiferromagnetic couplings.

The copper(II) derivative shows no SCM behavior, in contrast to what occurs in the cobalt(II) case, with the lower magnetic anisotropy of the Cu^{II} ions compared to that of the high-spin Co^{II} ion accounting for this feature. Magnetic measurements on polycrystalline samples of the $[Fe^{III}Co^{II}]$ chain show the occurrence of a *M* vs *H* hysteresis loop of a soft magnet (Figure 10a) and the frequency-dependent alternating current (ac) signals of a SCM (Figure 10b). A detailed study with the micro-SQUID technique on single

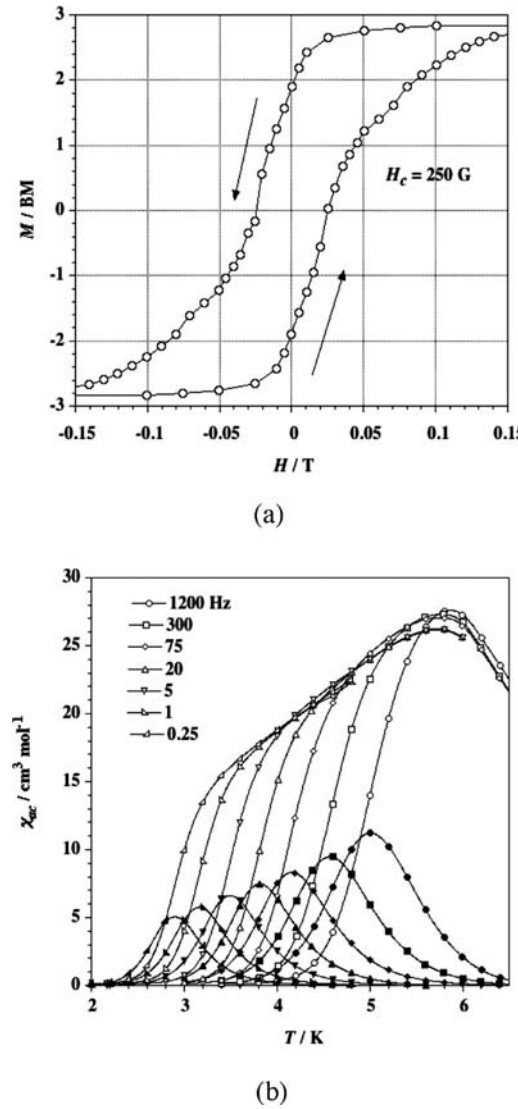

Figure 10. (a) Hysteresis loop of $\{[Fe^{III}(bpym)(CN)_4]_2Co^{II}(H_2O)_2\}\cdot 6H_2O$ at 2.0 K: (○) experimental data; (—) eye guide line. (b) In-phase (open symbols) and out-of-phase (full symbols) components of the ac susceptibility at $T \leq 6.4$ K in a 1 Oe field oscillating at different frequencies (0.25−1200 Hz) without a dc magnetic field.[36e]

crystals showed typical smooth hysteresis loops that are strongly temperature- and field-sweep-rate-dependent (Figure 11).

The slow relaxation of the magnetization of this chain was investigated with the ac magnetic susceptibility at high temperatures, whereas the relaxation measurements were used to extract the relaxation times at lower temperatures because of the slowness of the relaxation rate in the very low temperature domain. Two regimes were observed when the ac and dc relaxation times were plotted into an Arrhenius plot as shown in Figure 12: (i) the thermal dependence of the relaxation times follows an Arrhenius law with an activation energy $\Delta_{\tau 1}/k_B = 61.4$ K and $\tau_0 = 7.9 \times 10^{-10}$ s for $T \geq 3.0$ K; (ii) at $T < 3.0$ K, a departure from this behavior occurs with a smaller activation energy ($\Delta_{\tau 2}/k_B =$ 37.8 K) and a somewhat greater preexponential factor (1.5×10^{-9} s). The crossover at ca. 3.0 K was interpreted as the manifestation of finite-size effects.[15] This interpretation is in line with the fact that the correlation length would become

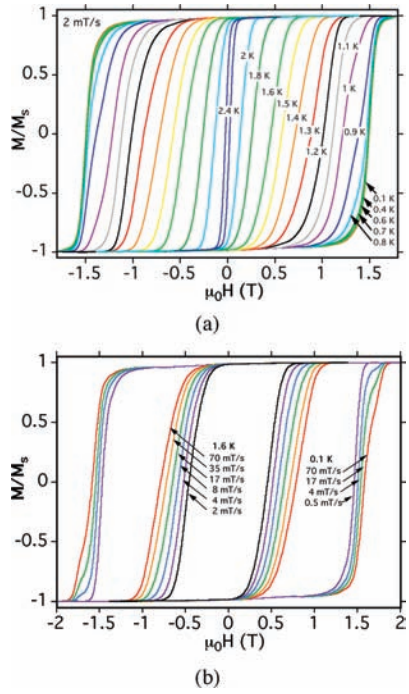

Figure 11. Hysteresis loops for an oriented single crystal of $\{[Fe^{III}(bpym)(CN)_4]_2Co^{II}(H_2O)_2\}\cdot 6H_2O$ at several temperatures and 2 mT/s (a) and at 0.1 and 1.6 K as a function of the sweep rate (b). The field is aligned with the easy axis of magnetization.[36e]

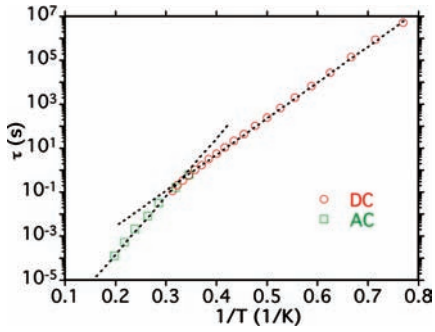

Figure 12. Semi-logarithm plot of τ against $1/T$ for $\{[Fe^{III}(bpym)(CN)_4]_2Co^{II}(H_2O)_2\}\cdot 6H_2O$: squares and circles are experimental data from ac susceptibility and dc decay measurements, respectively. The dotted lines are least-squares fits to the Arrhenius law.[36e]

very long at low temperatures and the occurrence of a very small number of defects would limit it. To conclude, this study of the slow relaxation of such a bimetallic chain shows that the dynamics is Glauber-like at high temperatures and that below 3.0 K a crossover to finite chain dynamics occurs. In addition, the quantum nucleation phenomenon[8b] was observed at very low temperatures.

Other examples of cyanide-bridged 4,2-ribbon-like $[Fe^{III}_2M^{II}]$ bimetallic chains are known (M = Cu and Ni).[36d,f,k,m] However, in most of them, the maximum of the frequency-dependent out-of-phase ac susceptibility occurs at very low temperatures. As illustrative examples, the blocking temperatures at 1000 Hz for the heterobimetallic chains $\{[Fe(HB(pz)_3)(CN)_3]Cu(MeOH)\}\cdot 2MeOH$ and $\{[Fe(HB(pz)_3)(CN)_3]Cu(DMF)\}\cdot DMF$ are 5.2 and 2.4 K, respectively.[36k,l] It is clear that the shift toward higher temperatures is one of the requirements to be achieved, keeping in mind the application of the SCMs in storing information, for instance.

III.3.2. Oxamato-Based SCMs. The synthetic strategy that we will summarize here is in part based on the crystal and magnetic engineering work that was performed by Kahn, Pei, and Lloret et al. in the 1990s dealing with solution−solid state studies on the complex formation between *N*,*N*′-bis(coordinating group substituted) oxamides/oxamates and transition-metal ions.[37−39] These studies showed that the *N*,*N*′-disubstituted oxamides are selective ligands for the Cu^{II} ions, leading to highly stable mono- and dinuclear oxamidato-containing copper(II) complexes. Their stability in solution,

(35) (a) Lescouëzec, R.; Lloret, F.; Julve, M.; Vaissermann, J.; Verdaguer, M. *Inorg. Chem.* **2002**, *41*, 818. (b) Toma, L. M.; Lescouëzec, R.; Toma, L. D.; Lloret, F.; Julve, M.; Vaissermann, J.; Andruh, M. *J. Chem. Soc., Dalton Trans.* **2002**, 3171. (c) Toma, L.; Toma, L. M.; Lescouëzec, R.; Armentano, D.; De Munno, G.; Andruh, M.; Cano, J.; Lloret, F.; Julve, M. *Dalton Trans.* **2005**, 1357. (d) Toma, L.; Lescouëzec, R.; Vaissermann, J.; Delgado, F. S.; Ruiz-Pérez, C.; Carrasco, R.; Cano, J.; Lloret, F.; Julve, M. *Chem.—Eur. J.* **2004**, *10*, 6130. (e) Zhang, Y.-Z.; Gao, S.; Wang, Z.-M.; Su, G.; Sun, H.-L.; Pan, F. *Inorg. Chem.* **2005**, *44*, 4534. (f) Lescouëzec, R.; Vaissermann, J.; Lloret, F.; Verdaguer, M. *Inorg. Chem.* **2002**, *41*, 5943. (g) Wang, S.; Zuo, J.-L.; Zhou, H.-C.; Choi, H.-J.; Ke, Y.; Long, J. R.; You, X.-Z. *Angew. Chem., Int. Ed.* **2004**, *43*, 5940. (h) Kim, J.; Han, S.; Cho, I.-K.; Choi, K.-Y.; Heu, M.; Yoon, S.; Su, B.-J. *Polyhedron* **2004**, *23*, 1333. (i) Kim, J.; Han, S.; Pokhodnya, K.; Migliori, J. M.; Miller, J. S. *Inorg. Chem.* **2005**, *44*, 6983. (j) Wang, S.; Zuo, J.-L.; Zhou, H.-C.; Song, Y.; You, X.-Z. *Inorg. Chim. Acta* **2005**, *358*, 2101. (k) Li, D.; Clérac, R.; Parkin, S.; Wang, G.; Yee, G. T.; Holmes, S. M. *Inorg. Chem.* **2006**, *45*, 5251. (l) Yang, J. Y.; Shores, M. P.; Sokol, J. J.; Long, J. R. *Inorg. Chem.* **2003**, *42*, 1403. (m) Rebilly, J. N.; Catala, L.; Charron, G.; Rogez, G.; Rivière, E.; Guillot, R.; Thuéry, P.; Barra, A. L.; Mallah, T. *Dalton Trans.* **2006**, 2818.

(36) (a) Toma, L.; Lescouëzec, R.; Vaissermann, J.; Herson, P.; Marvaud, V.; Lloret, F.; Julve, M. *New J. Chem.* **2005**, *29*, 210. (b) Lescouëzec, R.; Vaissermann, J.; Ruiz-Pérez, C.; Lloret, F.; Carrasco, R.; Julve, M.; Verdaguer, M.; Dromzée, Y.; Gatteschi, D.; Wernsdorfer, W. *Angew. Chem., Int. Ed.* **2003**, *42*, 1483. (c) Toma, L. M.; Lescouëzec, R.; Lloret, F.; Julve, M.; Vaissermann, J.; Verdaguer, M. *Chem. Commun.* **2003**, 1850. (d) Toma, L. M.; Delgado, F. S.; Ruiz-Pérez, C.; Carrasco, R.; Cano, J.; Lloret, F.; Julve, M. *Dalton Trans.* **2004**, 2836. (e) Toma, L. M.; Lescouëzec, R.; Pasán, J.; Ruiz-Pérez, C.; Vaissermann, J.; Cano, J.; Carrasco, R.; Wernsdorfer, W.; Lloret, F.; Julve, M. *J. Am. Chem. Soc.* **2006**, *128*, 4842. (f) Toma, L. M.; Lescouëzec, R.; Uriel, S.; Llusar, R.; Ruiz-Pérez, C.; Vaissermann, J.; Lloret, F.; Julve, M. *Dalton Trans.* **2007**, 3690. (g) Visinescu, D.; Toma, L. M.; Lloret, F.; Fabelo, O.; Ruiz-Pérez, C.; Julve, M. *Dalton Trans.* **2008**, 4103. (h) Lescouëzec, R.; Vaissermann, J.; Toma, L. M.; Carrasco, R.; Lloret, F.; Julve, M. *Inorg. Chem.* **2004**, *43*, 2234. (i) Wen, H.-R.; Wang, C.-F.; Zuo, J. L.; Song, Y.; Zeng, X.-R.; You, X.-Z. *Inorg. Chem.* **2006**, *45*, 582. (j) Wang, S.; Zuo, J.-L.; Zhou, H.-C.; Song, Y.; Gao, S.; You, X.-Z. *Eur. J. Inorg. Chem.* **2004**, 3681. (k) Wang, S.; Zuo, J.-L.; Gao, S.; Song, Y.; Zhou, H.-C.; Zhang, Y.-Z.; You, X.-Z. *J. Am. Chem. Soc.* **2004**, *126*, 8900. (l) Wen, H. R.; Wang, C.-F.; Song, Y.; Zuo, J.-L.; You, X.-Z. *Inorg. Chem.* **2006**, *45*, 8942. (m) Costa, V.; Lescouëzec, R.; Vaissermann, J.; Herson, P.; Journaux, Y.; Araujo, M. H.; Clemente-Juan, J. M.; Lloret, F.; Julve, M. *Inorg. Chim. Acta* **2008**, *361*, 3912.

(37) (a) Kahn, O. *Adv. Inorg. Chem.* **1995**, *43*, 179. and references cited therein. (b) Kahn, O., Ed. *Magnetism: A Supramolecular Function*; NATO ASI Series C; Kluwer: Dordrecht, Germany, 1996; Vol. 848.

(38) Ruiz, R.; Faus, J.; Lloret, F.; Julve, M.; Journaux, Y. *Coord. Chem. Rev.* **1999**, *193−195*, 1069.

(39) (a) Lloret, F.; Julve, M.; Faus, J.; Journaux, Y.; Philoche-Levisalles, M.; Jeannin, Y. *Inorg. Chem.* **1989**, *28*, 3702. (b) Lloret, F.; Sletten, J.; Ruiz, R.; Julve, M.; Faus, J.; Verdaguer, M. *Inorg. Chem.* **1992**, *31*, 778. (c) Lloret, F.; Julve, M.; Faus, J.; Ruiz, R.; Castro, I.; Mollar, M.; Philoche-Levisalles, M. *Inorg. Chem.* **1992**, *31*, 784. (d) Lloret, F.; Julve, M.; Real, J. A.; Faus, J.; Ruiz, R.; Mollar, M.; Castro, I.; Bois, C. *Inorg. Chem.* **1992**, *31*, 2956. (e) Soto, J.; Martínez-Máñez, R.; Payá, J.; Lloret, F.; Julve, M. *Transition Met. Chem.* **1993**, *18*, 69. (f) Real, J. A.; Mollar, M.; Ruiz, R.; Faus, J.; Lloret, F.; Julve, M.; Philoche-Levisalles, M. *J. Chem. Soc., Dalton Trans.* **1993**, 1483. (g) Real, J. A.; Ruiz, R.; Faus, J.; Lloret, F.; Julve, M.; Journaux, Y.; Philoche-Levisalles, M.; Bois, C. *J. Chem. Soc., Dalton Trans.* **1994**, 3769. (h) Sanz, J. L.; Cervera, B.; Ruiz, R.; Bois, C.; Faus, J.; Lloret, F.; Julve, M. *J. Chem. Soc., Dalton Trans.* **1996**, 1359.

good coordinating properties and the remarkable ability of the oxamidate/oxamate ligand to mediate strong magnetic interactions between the magnetic centers when acting as a bridge,[40] together with the great variety of *N,N′*-substituents that can be used, make them suitable and versatile building blocks for metal assembly in the field of molecular magnetism.

As an extension of the pioneering work by Kahn's group on the oxamidato-based magnetic compounds, Pardo et al. have explored a (poly)oxamato-based rational approach to high-nuclearity and high-dimensionality coordination polymers.[41] Special attention has to be paid to aspects such as the metalloligand precursor (substitution pattern and steric requirements of the bridging ligand) and the coordinated metal ion or metal complex (electronic configuration and local anisotropy).

Having in mind the rational design of oxamato-based SCMs, mononuclear copper(II) complexes with the ligands *N*-2-methylphenyloxamate (pmaMe), *N*-2,6-dimethylphenyloxamate ($pmaMe_2$), and *N*-2,4,6-trimethylphenyloxamate ($pmaMe_3$) were prepared (Scheme 2, top). In fact, these sterically hindered dianionic oxamatocopper(II) complexes, $[CuL_2]^{2-}$ (L = pmaMe, $pmaMe_2$, and $pmaMe_3$), can act as bis-bidentate ligands toward fully solvated, divalent transition-metal cations like Mn^{II} and Co^{II} because of their potential metal-binding ability through the two outer *cis*-carbonyl O atoms of the oxamato groups. This "complex-as-ligand" approach results in oxamato-bridged heterobimetallic chains, with three possible structures being envisaged: (i) a linear chain is obtained when the solvent molecules coordinate to the M^{II} ions (M = Mn and Co) in *trans* positions (Scheme 2a);[42a,b] (ii and iii) zigzag[42c] or helical structures may result when they coordinate in *cis* positions, as a function of the steric requirements of the copper(II) precursor (parts b and c of Scheme 2, respectively). The resulting 1D coordination compounds would behave as well-isolated oxamato-bridged bimetallic chains because of the sterically hindered nature of this family of methyl-substituted phenyloxamate bridging ligands filling thus one of the required conditions to exhibit SCM behavior. In addition, these polymethyl-substituted phenyloxamate ligands offer the possibility of investigating the influence of weak interchain interactions on the relaxation dynamics of the magnetization for this family of 1D compounds in a systematic way.[43] Thus, the variation in the number and substitution pattern of the methyl substituents would allow a study of the intercrossing between short- (nanoscopic) and long-range (macroscopic) magnetic behaviors.

Scheme 2

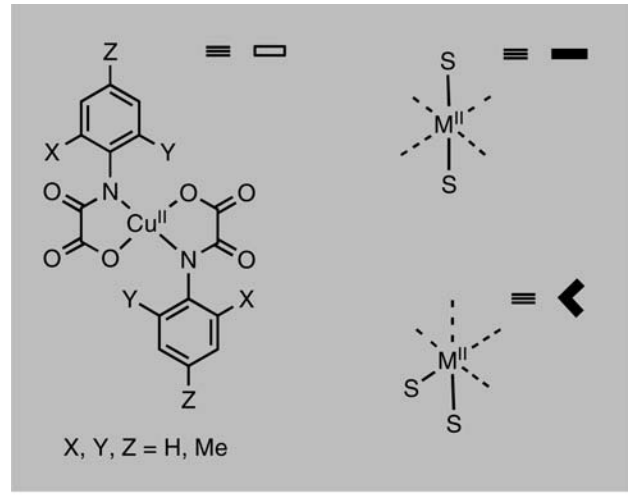

The reaction of the sodium salts of the precursor $[CuL_2]^{2-}$ (L = pmaMe, $pmaMe_2$, and $pmaMe_3$) with $Co(NO_3)_2 \cdot 6H_2O$ in either DMSO or water afforded the neutral bimetallic chains of the general formula $Co^{II}Cu^{II}L_2 \cdot nS$ (S = DMSO or H_2O).[44] Within each chain, the dianionic copper(II) entity acts as bis-bidentate ligand through the *cis*-carbonyl O atoms of the oxamato groups toward the divalent metal cations. They have either zigzag or linear 1D architectures according to whether the two solvent molecules are coordinated to the octahedral Co^{II} ions in *cis* and *trans* positions, as illustrated by the crystal structures of $[CoCu(pmaMe_2)_2(H_2O)_2]$ (Figure 13a) and $[CoCu(pmaMe_3)_2(H_2O)_2] \cdot 4H_2O$ (Figure 14a).[44] In the former case, the regular alternation of enantiomers of opposite propeller chirality (Δ and Λ) for the *cis*-diaqua Co^{II} ions leads to the overall achiral zigzag chain structure. In both structures, the chains are rather well-separated from each other in the crystal lattice because of the presence of the bulky methyl-substituted phenyl groups (Figures 13b and 14b, respectively). There are weak interchain hydrogen-bonding interactions involving the coordinated water mol-

(40) Cano, J.; Ruiz, E.; Alemany, P.; Lloret, F.; Alvarez, S. *J. Chem. Soc., Dalton Trans.* **1999**, 1669.

(41) Pardo, E.; Ruiz-García, R.; Cano, J.; Ottenwaelder, X.; Lescouëzec, R.; Journaux, Y.; Lloret, F.; Julve, M. *Dalton Trans.* **2008**, 2780. and references cited therein. .

(42) (a) Stumpf, H. O.; Pereira, C. L. M.; Doriguetto, A. C.; Konzen, C.; Meira, L. C. B.; Fernandes, N. G.; Mascarenhas, Y. P.; Ellena, J.; Knobel, M. *Eur. J. Inorg. Chem.* **2005**, *24*, 5018. (b) Stumpf, H. O.; Pei, Y.; Ouahab, L.; Leberre, F.; Codjovi, E.; Kahn, O. *Inorg. Chem.* **1993**, *32*, 5687. (c) Stumpf, H. O.; Pei, Y.; Kahn, O.; Sletten, J.; Renard, J. P. *J. Am. Chem. Soc.* **1993**, *115*, 6738.

(43) (a) Mydosh, J. A. *Spin Glasses: An Experimental Introduction*; Taylor & Francis: London, 1993. (b) Girtu, M. A.; Wynn, C. M.; Fujita, W.; Awaga, K.; Epstein, A. *Phys. Rev. B* **1998**, *57*, R11058.

(44) (a) Pardo, E.; Ruiz-García, R.; Lloret, F.; Faus, J.; Julve, M.; Journaux, Y.; Delgado, F. S.; Ruiz-Pérez, C. *Adv. Mater.* **2004**, *16*, 1597. (b) Pardo, E.; Ruiz-García, R.; Lloret, F.; Faus, J.; Julve, M.; Journaux, Y.; Novak, M. A.; Delgado, F. S.; Ruiz-Pérez, C. *Chem.—Eur. J.* **2007**, *13*, 2054.

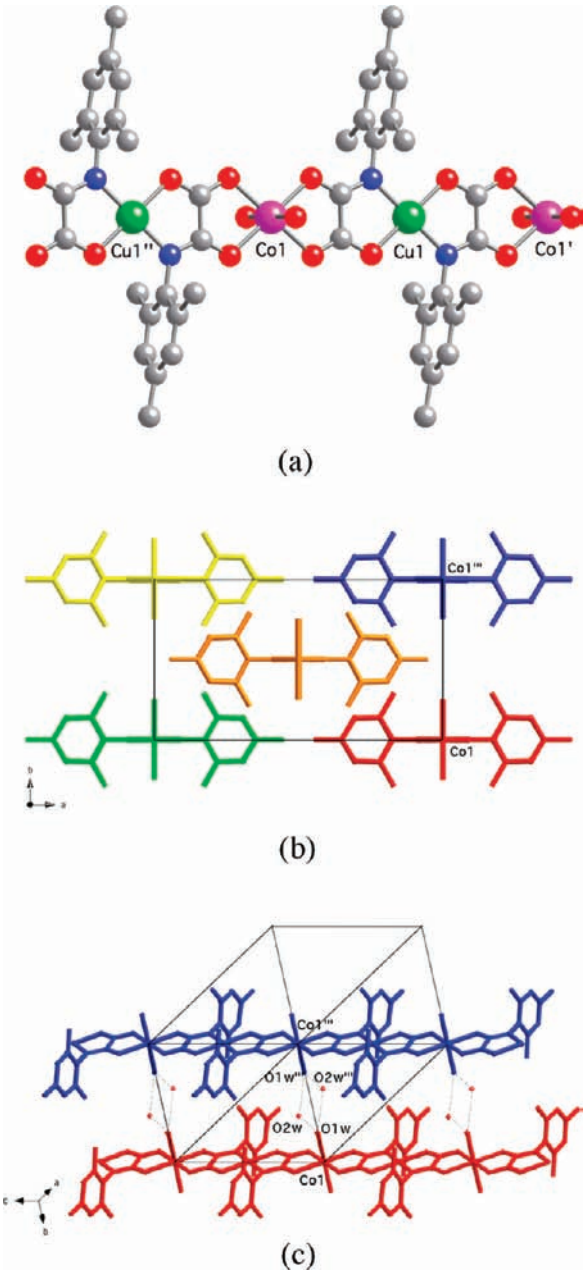

Figure 13. (a) Perspective view of a fragment of the zigzag chain of $[CoCu(pmaMe_2)_2(H_2O)_2]$ with the atom numbering of the metal environments (the H atoms have been omitted for clarity). (b and c) Drawings of the crystal packing of the chains along the [10−1] and [101] directions, respectively (hydrogen bonds are represented by dashed lines). Symmetry codes: I = $^1/_2 - x$, $^1/_2 - y$, $-z$; II = $-x$, y, $^1/_2 - z$; III = x, $1 - y$, $1 - z$. Reproduced with permission of 44b. Copyright Wiley-VCH Verlag GmbH & Co. KGaA.

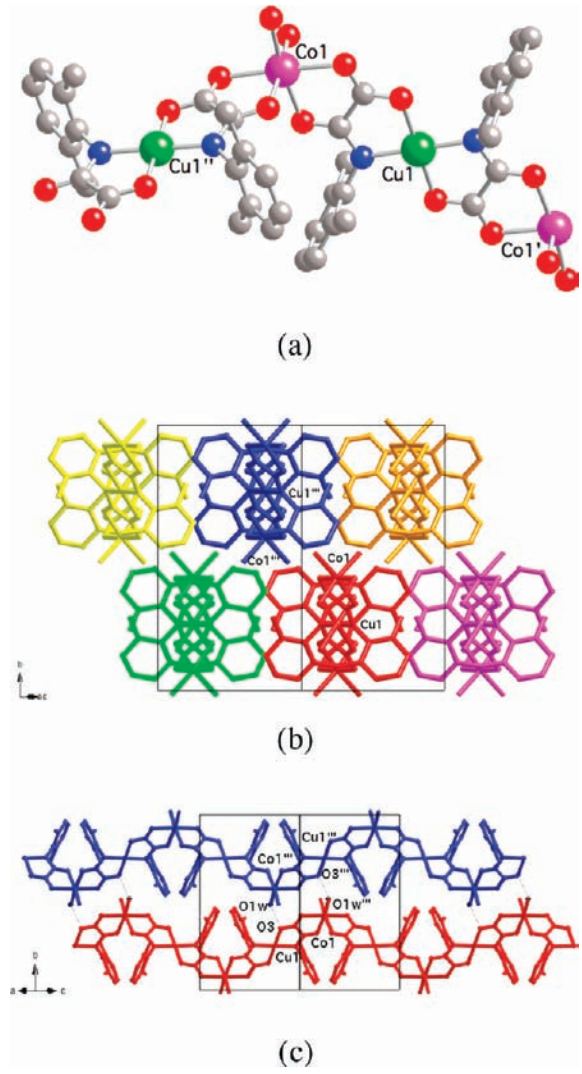

Figure 14. (a) Perspective view of a fragment of the zigzag chain of $[CoCu(pmaMe_3)_2(H_2O)_2]\cdot 4H_2O$ with the atom numbering of the metal environments (the H atoms have been omitted for clarity). (b and c) Drawings of the crystal packing of the chains along the [001] and [111] directions, respectively (hydrogen bonds are represented by dashed lines). Symmetry codes: I = $-x$, y, $-z$; II = $-x$, y, $1 - z$; III = x, $1 + y$, z. Reproduced with permission of 44b. Copyright Wiley-VCH Verlag GmbH & Co. KGaA.

ecules and either the carbonyl O atoms from the oxamate bridging groups in the former compound or the crystallization water molecules in the latter one (Figures 13c and 14c, respectively). The values of the intrachain Cu···Co distance through the oxamate bridge are very close in the two compounds [5.296(1) and 5.301(2) Å], while the shortest interchain Co···Co separations through the two-atom [O_w···O(oxamato)] or four-atom [$(O_w)_4$ ring] pathway are 5.995(5) and 8.702(3) Å, respectively.

The magnetic properties of this series of heterobimetallic compounds $Co^{II}Cu^{II}L_2\cdot n$S with sterically hindered polymethyl-substituted phenyloxamate (L) as bridging ligands are characteristic of ferrimagnetically organized chains (occurrence of a minimum in the χT vs T plot) with slow relaxation of the magnetization at low temperatures ($T_B > 3.5$ K at $\nu = 1$ Hz) typical of SCMs. In fact, the saturation magnetization (per $Co^{II}Cu^{II}$ unit) at 2.0 K varies in the range 0.98−1.10 μ_B, values that are consistent with the predicted ones for the antiparallel alignment of the spins of Co^{II} ($S_{Co} = S_{eff} = ^1/_2$) and Cu^{II} ($S_{Cu} = ^1/_2$) ions ($M_s = (g_{Co}S_{Co} - g_{Cu}S_{Cu})N\mu_B = 1.10\ \mu_B$ with $g_{Co} = 4.3$ and $g_{Cu} = 2.1$).

The relatively large intrachain antiferromagnetic coupling between the Cu^{II} and high-spin Co^{II} ions in this family [$J/k_B = -25.2$ to -32.9 K (-17.5 to -22.9 cm^{-1}) with $\mathbf{H} = \Sigma_i[-2J\boldsymbol{S}_{Co,i(z)}\cdot\boldsymbol{S}_{Cu,i(z)} - (3/2)k\lambda\boldsymbol{L}_{Co,i(z)}\cdot\boldsymbol{S}_{Co,i(z)} + D\boldsymbol{L}_{Co,i(z)}^2 - \beta H_{(z)}(g_{Co}\boldsymbol{S}_{Co,i(z)} + g_{Cu}\boldsymbol{S}_{Cu,i(z)} + k\boldsymbol{L}_{Co,i(z)})]$ being $S_{Co} = ^3/_2$, $L_{Co} = 1$, and $S_{Cu} = ^1/_2$] is related to the fact that the Cu atom is coplanar with the oxamato plane, as shown by the crystal structures of $[CoCu(pmaMe_2)_2(H_2O)_2]$ and $[CoCu(pmaMe_3)_2$-

$(H_2O)_2]\cdot 4H_2O$.[42a,44] The somewhat reduced values of both the orbital reduction factor k (ca. 0.80−0.98) and the spin−orbit coupling λ [$\lambda/k_B = -118$ to $+158$ K (-82 to -110 cm^{-1})] parameters for the high-spin octahedral Co^{II} ion reveal a moderate covalency of the Co−O bonds (to be compared with $k = 1$ and $\lambda_0 = -259$ K or -180 cm^{-1} for the free ion), which is ultimately responsible for the strong spin delocalization on the oxamato bridge. Otherwise, the large values of the axial magnetic anisotropy parameter D [$D/k_B = 774-1034$ K (538−719 cm^{-1})], which is related to the zero-field splitting of the orbital triplet $^4T_1$ ground state of the high-spin Co^{II} ion, indicate an important axial distortion of the octahedral metal environment.

The values of the blocking temperature along this series, calculated as the temperature of the maxima of χ'' ($T_B = T_{max}$ for $\nu = 1-1000$ Hz) whereby it is assumed that the switching of the oscillating ac field matches the relaxation rate of the magnetization ($1/\tau = 2\pi\nu$), follow the steric hindrance of both the aromatic group-substituted oxamate ligand (pmaMe < $pmaMe_2$ < $pmaMe_3$) and the coordinated solvent molecules (H_2O < DMSO). It appears that the interchain interactions may tune the dynamic magnetic properties by lowering the blocking temperature with respect to that expected for a perfectly isolated chain. Although the relevance of this hypothesis still has to be supported with new experimental and theoretical works, we guess that the implications that can be derived from it may be a subject of discussion in the context of the proposed mechanisms for the slow magnetic relaxation of SCMs in the years to come.

The analysis of the SCM behavior of $CoCu(pmaMe_3)_2(DMSO)_3$ and $[CoCu(pmaMe_3)_2(H_2O)_2]\cdot 4H_2O$ on the basis of Glauber's theory for an Ising 1D system shows a thermally activated mechanism for the magnetic relaxation (Arrhenius law's dependence; Figure 15a).[44b] The values of the activation energy (Δ_τ/k_B) are 54.7 (S = DMSO) and 23.5 K (S = H_2O), while those of the preexponential factor (τ_0) are 2.3×10^{-11} (S = DMSO) and 4.0×10^{-9} s (S = H_2O). As expected, the larger the antiferromagnetic intrachain coupling [$J/k_B = -63.7$ (S = DMSO) and -50.3 K (S = H_2O)] and the axial Ising-type magnetic anisotropy [$D/k_B = 1021$ K or 710 cm^{-1} (S = DMSO) and 878 K or 610 cm^{-1} (S = H_2O)] are, the greater the activation energy for the magnetization reversal is, as observed experimentally. Indeed, the χ_M'' vs χ_M' plot (known as the Cole−Cole plot) at 2.0 K in the frequency range 1−1400 Hz gives a rather symmetric semicircle in both cases according to the generalized Debye expression $\chi_M'' = (\chi_S - \chi_T)\tanh[\alpha\pi/2]/2 + \{(\chi_M' - \chi_S)(\chi_T - \chi_M') + (\chi_T - \chi_S)^2\tanh^2[\alpha\pi/2]/4\}^{1/2}$ (Figure 15b). The values for the α parameter are 0.10 (S = DMSO) and 0.05 (S = H_2O) (α is equal to 0 for an ideal Debye model with a single relaxation time), discarding thus a spin-glass behavior that would result from a large intrachain segment size dispersion and/or interchain interactions. Moreover, the F parameter, which takes account of the relative variation of the temperature of the maximum of χ_M'' with respect to the frequency,[43a] is equal to 0.25 (S = DMSO) and 0.12 (S = H_2O). These moderate F values are typical of SCMs, and they are greater than those expected for spin glasses (F values lower than 0.01).[45]

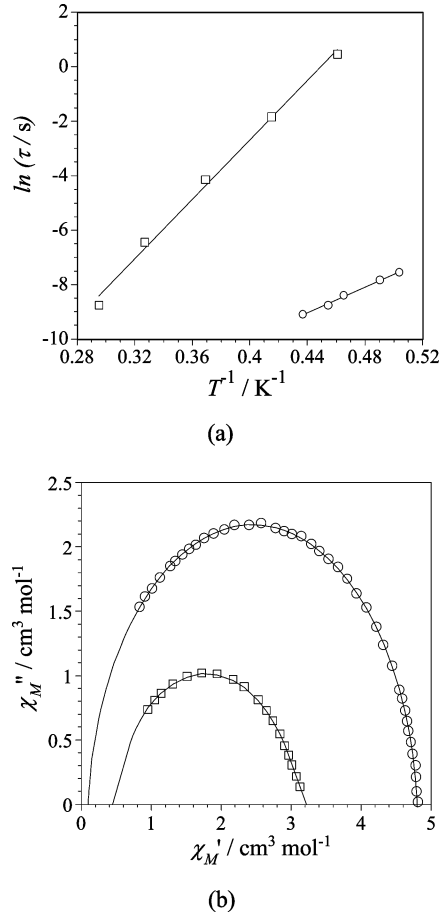

Figure 15. (a) Arrhenius and (b) Cole−Cole plots at 2.0 K for $CoCu(pmaMe_3)_2\cdot 3DMSO$ (squares) and $[CoCu(pmaMe_3)_2(H_2O)_2]\cdot 4H_2O$ (circles). Reproduced with permission of 44b. Copyright Wiley-VCH Verlag GmbH & Co. KGaA.

The SCM behavior for this family of oxamato-bridged $[Co^{II}Cu^{II}]$ chains obeys the large Ising-type magnetic anisotropy within the chain and the minimization of the interchain interactions, which result from the combination of an orbitally degenerate high-spin octahedral Co^{II} ion ($^4T_1$) and a square-planar Cu^{II} complex with such a bulky methyl-group-substituted phenyloxamate ligand. The corresponding oxamato-bridged $[Mn^{II}Cu^{II}]$ compounds are also ferrimagnetically organized chains, but they showed no evidence of slow magnetic relaxation effects.[44b] This is most likely due to the isotropic character of the octahedral high-spin Mn^{II} ion ($^6A_{1g}$ term with a D value practically zero). The search for related mononuclear copper(II) precursors with long alkyl- or aryl-group-substituted phenyloxamate ligands of even larger steric hindrance in order to obtain perfectly well-isolated oxamato-bridged heterobimetallic chains as potential candidates to high-T_B SCMs will be one of the tasks to be accomplished in the near future.

III.4. Other Approaches to the Design of SCMs. SMM properties have been obtained serendipitously in many homometallic (same element with different oxidation states) and heterometallic complexes and therefore similarly, self-

(45) Binder, K.; Young, A. P. *Rev. Mod. Phys.* **1986**, *58*, 801.

assembly reactions of metal sources with bridging and capping ligands (or solvents) may produce serendipitously chains exhibiting SCM behavior.[46] Indeed, this is possible even for metal ions that possess easy-plane anisotropy ($D > 0$). Kajiwara and co-workers have synthesized an alternating chain made of high-spin Fe^{II} ($S = 2$) and low-spin Fe^{III} ($S = {}^1/_2$) ions where the high-spin Fe^{II} ion in an elongated octahedral geometry possesses easy-plane (equatorial) anisotropy on the $^5B_{2g}$ ground state.[47] At first sight, this compound looks like a typical Heisenberg chain. However, because of an orthogonally twisted arrangement of the easy plane of the Fe^{II} moiety through the Fe^{III} ion, the magnetic interaction leads at low temperatures to a uniaxial spin arrangement along the chain direction. This compound exhibited slow relaxation of the magnetization, i.e., SCM behavior; however, the mechanism of the observed relaxation dynamics has not yet been fully understood as in other ferrimagnetically arranged chains.

IV. Perspectives and Open Questions

We mentioned in the introduction that the limitation to produce SCMs compatible with industrial applications seems less severe than that for SMMs. Is it really possible to create such SCMs working at high temperature? This question as well as the design of multifunctional SCMs (optically active, photoswitching, redox activity, spin-crossover, electrical conduction, etc.) has no answer at the moment, but one can say that it is within the odds. The versatility of some of the precursors shown in the preceding sections (in the case of the manganese(III) Schiff base and the cyano- or oxamato-bearing complexes) makes them suitable systems to prepare multifunctional SCMs in the near future. Apart from this mainly chemical work, we currently have a good number of fundamental questions on SCMs to be clarified whose answers would consequently open a route to high-temperature SCMs. Some of these questions are quoted here: (i) What about the relaxation mechanism in SCMs that exhibit a strong intrachain interaction beyond the Ising limit ($|D/J| << {}^4/_3$)? (ii) How can we treat theoretically the relaxation dynamics in alternating heterospin chains? (iii) How can we see the boundary between SCMs as isolated chains and bulk magnetism and what are the phenomena involved at the frontier? (iv) Finally, can we use the interchain interactions as a perturbation for SCMs? Considering the fundamental questions (iii) and (iv), the materials might not exhibit any more SCM properties, but it might add a fresh dimension to creating new magnetic materials based on SCM systems. Recently, an interesting result was reported by Ishida et al., who found that a cobalt(II)−organic radical chain exhibits unprecedented M vs H hysteresis with a giant coercive field up to 5 T at 6 K and relatively high temperature relaxation, for example, $T_B = 15$ K at 10 Hz ac frequency.[48] Then, Sessoli reported her idea that the intrinsic slow relaxation behavior of component anisotropic chains, like Glauber dynamics, is a key to creating hard magnets with large coercive fields.[49] Thus, control of the interchain interactions might be a trigger to preparing SCM-based magnetic materials.

Since the discovery of SCM at the beginning of this century, many examples of SCMs and their related compounds have been synthesized. Some of them have been theoretically understood in terms of their static and dynamic properties. However, a lot of questions and parameters to play on remain that require joint works and discussions between chemists and physicists. In conclusion, it is clear that SCMs are a wide and open gateway to new magnetic materials in the near future.

V. Experimental Section

Synthesis. All synthetic procedures were carried out under aerobic conditions at room temperature. All chemicals and solvents used during the syntheses were reagent grade and used as received. $[Mn_2(saltmen)_2(H_2O)_2](PF_6)_2 \cdot 2H_2O$,[50] $[Ni(pao)_2(bpy)] \cdot n(solvent)$, and $[Ni(pao)_2(phen)] \cdot n(solvent)$[51] were prepared according to the literature methods.

$[Mn_2(saltmen)_2Ni(pao)_2(L)](PF_6)_2$ (L = bpy, 1; phen, 2). A 20 mL methanol solution containing $[Mn_2(saltmen)_2(H_2O)_2](PF_6)_2 \cdot 2H_2O$ (141 mg, 0.125 mmol) and a 10 mL methanol solution of $[Ni(pao)_2(bpy)] \cdot 2H_2O$ (122 mg, 0.25 mmol) for **1** or $[Ni(pao)_2(phen)] \cdot 2.5CHCl_3$ (194 mg, 0.25 mmol) for **2** were prepared in different batches and divided into five portions, respectively, to fill up narrow-diameter glass tubes (∅: 8 mm) for slow diffusion crystallization. In these crystallization experiments, the lower and upper layers are the nickel (2 mL) and manganese (4 mL) precursor solutions, respectively. The five sealed tubes were kept undisturbed at room temperature until the diffusions were completed (about 3 weeks). Dark-brown block-type crystals of the desired compound were collected by suction filtration, washed with methanol, and dried in air. Yield (based on Mn): 75−80%. Elem anal. Calcd for $\mathbf{1} \cdot 2H_2O$ (found): C, 48.43 (48.47); H, 4.33 (4.35); N, 9.11 (9.18). IR (KBr, cm^{-1}): ν(C═N) 1604, ν(P−F) 843, δ(−F−P−F), 559. Elem anal. Calcd for $\mathbf{2} \cdot 1.25H_2O$ (found): C, 49.65 (49.72); H, 4.20 (4.23); N, 9.05 (9.14). IR (KBr, cm^{-1}): ν(C═N) 1604, ν(P−F) 845, δ(−F−P−F) 559.

Physical Measurements. IR spectra were measured on KBr disks with a Jasco FT-IR 620 spectrophotometer. Magnetic susceptibility measurements were obtained with the use of a Quantum Design SQUID magnetometer MPMS-XL. dc measurements were collected from 1.8 to 300 K and from −70 to +70 kOe. ac measurements were performed at various frequencies from 1 to 1488 Hz with an ac field amplitude of 3 Oe and no dc field applied. The general measurements were performed on finely ground polycrystalline samples. Experimental data were also corrected for the sample holder and for the diamagnetic contribution calculated from Pascal

(46) (a) Liu, T. F.; Fu, D.; Gao, S.; Zhang, Y. Z.; Sun, H. L.; Su, G.; Liu, Y. J. *J. Am. Chem. Soc.* **2003**, *125*, 13976. (b) Sun, Z. M.; Prosvirin, A. V.; Zao, H. H.; Mao, J. G.; Dunbar, K. R. *J. Appl. Phys.* **2005**, *97*, 10B305.
(47) Kajiwara, T.; Nakano, M.; Kaneko, Y.; Takaishi, S.; Ito, T.; Yamashita, M.; Kamiyama, A. I.; Nojiri, H.; Ono, Y.; Kojima, N. *J. Am. Chem. Soc.* **2005**, *127*, 10150.
(48) Ishii, N.; Okamura, Y.; Chiba, S.; Nogami, T.; Ishida, T. *J. Am. Chem. Soc.* **2008**, *130*, 24.
(49) Sessoli, R. *Angew. Chem., Int. Ed.* **2008**, *47*, 5508.
(50) Miyasaka, H.; Clérac, R.; Ishii, T.; Chang, H.-C.; Kitagawa, S.; Yamashita, M. *J. Chem. Soc., Dalton Trans.* **2002**, 1528.
(51) Miyasaka, H.; Furukawa, S.; Yanagida, S.; Sugiura, K.; Yamashita, M. *Inorg. Chim. Acta* **2004**, *357*, 1619.

constants.[52] Single-crystal magnetic measurements were performed on the same apparatus using a horizontal rotator attachment. The single crystal of dimensions 1.4 × 0.9 × 0.5 mm used for the measurements was fixed at a platform of the rotator by an Apiezon-N grease.

X-ray Crystallography. Single crystals of **1** and **2** were mounted on glass rods. The crystal dimensions were 0.21 × 0.18 × 0.15 mm for **1** and 0.13 × 0.10 × 0.08 mm for **2**. Data collections were taken on a Rigaku CCD diffractometer (Saturn70) with graphite-monochromated Mo Kα radiation ($\lambda = 0.710\ 70$ Å). The structures were solved by heavy-atom Patterson methods[53] and expanded using Fourier techniques (*DIRDIF99*).[54] The non-H atoms were refined anisotropically, except for crystallization solvent molecules that were refined isotropically. The H atoms were introduced as fixed contributors. Full-matrix least-squares refinements on F^2 converged with unweighted and weighted agreement factors of R1 $= \sum||F_o| - |F_c||/\sum|F_o|$ ($I > 2.00\sigma(I)$ and all data) and wR2 $= [\sum w(F_o^2 - F_c^2)^2/\sum w(F_o^2)^2]^{1/2}$ (all data). Sheldrick's weighting scheme was used. All calculations were performed by using the *CrystalStructure* crystallographic software package.[55] CCDC 705676 for **1** and CCDC 705677 for **2** contain the supplementary crystallographic data for this paper. These data can be obtained free of charge from The Cambridge Crystallographic Data Centre via www.ccdc.cam.ac.uk/data_request/cif.

(52) Boudreaux, E. A., Mulay, L. N., Eds. *Theory and Applications of Molecular Paramagnetism*; John Wiley & Sons: New York, 1976.
(53) PATTY: Beurskens, P. T.; Admiraal, G.; Beurskens, G., Bosman, W. P.; Garcia-Granda, S.; Gould, R. O.; Smits, J. M. M.; Smykalla, C. *The DIRDIF program system, Technical Report of the Crystallography Laboratory*; University of Nijmengen: Nijmengen, The Netherlands, 1992.
(54) DIRDIF99: Beurskens, P. T., Admiraal, G.; Beurskens, G., Bosman, W. P., de Gelder, R.; Israel, R., Smits, J. M. M. *The DIRDIF-99 program system, Technical Report of the Crystallography Laboratory*; University of Nijmengen: Nijmengen, The Netherlands, 1999.
(55) *CrystalStructure 3.8: Crystal Structure Analysis Package*; Rigaku and Rigaku Americas: The Woodlands TX, 2000−2007.

Crystal data for $1\cdot H_2O$: $C_{62}H_{64}N_{10}O_7P_2F_{12}Mn_2Ni$, fw = 1519.75, monoclinic $P2_1/n$ (No. 14), $T = 93 \pm 1$ K, λ(Mo Kα) = 0.710 70 Å, $a = 16.810(4)$ Å, $b = 20.638(4)$ Å, $c = 19.855(4)$ Å, $\beta = 106.504(3)°$, $V = 6604(2)$ Å^3, $Z = 4$, $D_{calc} = 1.528$ g/cm^3, $F_{000} = 3112.00$, $\mu = 8.008$ cm^{-1}, $2\theta_{max} = 50.0°$. Final R1 = 0.0675 [$I > 2.00\sigma(I)$], R1 = 0.1398 (all data), wR2 = 0.2035 (all data), GOF = 1.018, $\rho_{max} = 1.13$ e/Å^3, $\rho_{min} = -0.47$ e/Å^3.

Crystal data for $2\cdot 1.25H_2O$: $C_{64}H_{64.5}N_{10}O_{7.25}P_2F_{12}Mn_2Ni$, fw = 1519.75, monoclinic $P2_1/n$ (No. 14), $T = 93 \pm 1$ K, λ(Mo Kα) = 0.710 70 Å, $a = 16.855(3)$ Å, $b = 20.274(3)$ Å, $c = 20.262(3)$ Å, $\beta = 107.2800(18)°$, $V = 6611.5(16)$ Å^3, $Z = 4$, $D_{calc} = 1.555$ g/cm^3, $F_{000} = 3170.00$, $\mu = 8.019$ cm^{-1}, $2\theta_{max} = 50.0°$. Final R1 = 0.0414 [$I > 2.00\sigma(I)$], R1 = 0.0633 (all data), wR2 = 0.1136 (all data), GOF = 1.003, $\rho_{max} = 0.58$ e/Å^3, $\rho_{min} = -0.41$ e/Å^3.

Acknowledgment. The authors thank all past and actual co-workers whose names appear in the references. Without their continuous hard work, creativity, and enthusiasm devoted to this hot topic of Molecular Magnetism, the present Forum Article would not be. The authors are also grateful to the European network MAGMANet (NMP3-CT-2005-515767), The EC-TMR Network QuEMolNa (MRTN-CT-2003-504880), the University of Bordeaux, the CNRS, the Région Aquitaine, the Spanish Ministry of Science and Education, the Consolider Ingenio 2010 (Molecular Nanoscience), CREST and PRESTO projects, Japan Science and Technology Agency (JST), and a Grant-in-Aid for Scientific Research from the Ministry of Education, Culture, Sports, Science, and Technology, Japan, for funding.

Supporting Information Available: X-ray crystallographic data in CIF format of **1** and **2**. This material is available free of charge via the Internet at http://pubs.acs.org.

IC802050J